SYNTHESIS AND ELECTROCHEMICAL PERFORMANCE OF HIGH ENTROPY OXIDES AS AN ANODE FOR LITHIUM-ION BATTERIES

A THESIS SUBMITTED TO
THE GRADUATE SCHOOL OF NATURAL AND APPLIED SCIENCES
OF
MIDDLE EAST TECHNICAL UNIVERSITY

BY

DENIZ OKAN BAYRAKTAR

IN PARTIAL FULFILLMENT OF THE REQUIREMENTS
FOR
THE DEGREE OF MASTER OF SCIENCE
IN
METALLURGICAL AND MATERIALS ENGINEERING

DECEMBER 2023

Approval of the thesis:

SYNTHESIS AND ELECTROCHEMICAL PERFORMANCE OF HIGH ENTROPY OXIDES AS AN ANODE FOR LITHIUM-ION BATTERIES

submitted by **DENIZ OKAN BAYRAKTAR** in partial fulfillment of the requirements for the degree of **Master of Science** i**n Metallurgical and Materials Engineering, Middle East Technical University** by,

Prof. Dr. Halil Kalıpçılar
Dean, Graduate School of **Natural and Applied Sciences** _____

Prof. Dr. Ali Kalkanlı
Head of the Department, **Metallurgical and Materials Eng.** _____

Assist. Prof. Dr. Çiğdem Toparlı
Supervisor, **METE, METU** _____

Assist. Prof. Dr. Ersu Lökçü
Co-Supervisor, **METE, ESOGU** _____

Examining Committee Members:

Prof. Dr. Kadri Aydınol
Metallurgical and Materials Eng, METU _____

Asst. Prof. Dr. Çiğdem Toparlı
Metallurgical and Materials Eng, METU _____

Prof. Dr. Tayfur Öztürk
Metallurgical and Materials Eng, METU _____

Assoc. Prof. Dr. Burak Ülgüt
Chemistry, Bilkent Uni. _____

Prof. Dr. Hüsnü Emrah Ünalan
Metallurgical and Materials Eng, METU _____

Date: 13.12.2023

I hereby declare that all information in this document has been obtained and presented in accordance with academic rules and ethical conduct. I also declare that, as required by these rules and conduct, I have fully cited and referenced all material and results that are not original to this work.

Name Last name : Deniz Okan Bayraktar

Signature :

ABSTRACT

SYNTHESIS AND ELECTROCHEMICAL PERFORMANCE OF HIGH ENTROPY OXIDES AS AN ANODE FOR LITHIUM-ION BATTERIES

Bayraktar, Deniz Okan
Master of Science, Metallurgical and Materials Engineering
Supervisor: Assist Prof. Dr. Çiğdem Toparlı
Co-Supervisor: Assist. Prof. Dr. Ersu Lökçü

December 2023, 63 pages

Lithium-ion batteries are indispensable part of our lives. Ever since their commercial applications the demand for higher performance is ever increasing. Increase in performance can be achieved by ingenious cell designs but the better performing active materials allows a bigger leap in the electrochemical performance. That is why industry and academia is in a perpetual race to achieve better performing products. One of such highly researched materials is high entropy oxides (HEO). High entropy oxides are demonstrating interesting properties both in terms of electrochemical and physical characteristics. One of the main objectives of this work is to investigate the lithium-ion diffusion properties and electrochemical properties dependance on the structure of the high entropy oxide material. For this reason, the effects of the synthesis environment of flowing argon and air on the structural and electrochemical properties of powders of $(FeMnCrCoZn)_3O_4$ high entropy oxides are investigated in this study. HEO synthesized in argon atmosphere (HEO-Ar) and the one synthesized in air (HEO-Air) were structurally and morphologically characterized. The increased electrochemical performance of HEO-Ar compared to HEO-Air has been shown. The oxygen vacancies, characterized by x-ray photoelectron spectroscopy method, in the HEO-Ar sample improve electrochemical performances by increasing the number of sites for Li^+ accommodation, increasing conductivity, and accelerating Li^+ diffusion kinetics. Both materials, although, having higher specific capacities,

demonstrate higher operating voltages compared to graphite. Knowing these properties gives both material designer and cell designer the ability to design materials and electrochemical cells according to the specific application of energy storage. Considering their enhanced current rate capabilities and extended cycle life these materials may possibly be used in grid level applications, such as peak shaving, grid support and renewable energy storage.

Keywords: Lithium-Ion Batteries, High Entropy Oxides, Anode

ÖZ

YÜKSEK ENTROPİLİ OKSİTLERİN ÜRETİMİ VE LİTYUM İYON BATARYALARDA KULLANIMI

Bayraktar, Deniz Okan
Yüksek Lisans, Metalurji ve Malzeme Mühendisliği
Tez Yöneticisi: Dr. Öğr. Üyesi Çiğdem Toparlı
Ortak Tez Yöneticisi: Dr. Öğr Üyesi Ersu Lökçü

Aralık 2023, 63 sayfa

Lityum-iyon piller hayatımızın vazgeçilmez bir parçası. Ticari uygulamalarından bu yana, daha yüksek performansa olan talep giderek artıyor. Performans artışı ustaca hücre tasarımlarıyla sağlanabilir ancak daha iyi performans gösteren aktif malzemeler, elektrokimyasal performansta daha büyük bir sıçramaya olanak tanır. Bu nedenle endüstri ve akademi, daha iyi performans gösteren ürünlere ulaşmak için sürekli bir yarış içindedir. Bu tür çok araştırılan malzemelerden biri Yüksek entropi oksitlerdir. Yüksek entropili oksitler hem elektrokimyasal hem de fiziksel özellikler açısından ilginç özellikler göstermektedir. Bu çalışmanın temel amaçlarından biri, yüksek entropili oksit malzemenin yapısına bağlı olarak lityum iyon difüzyon özelliklerini ve elektrokimyasal özellikleri araştırmaktır. Bu nedenle bu çalışmada argon ve hava sentez ortamının (FeMnCrCoZn)3O4 yüksek entropili oksit (HEO) tozlarının yapısal ve elektrokimyasal özellikleri üzerine etkileri araştırılmıştır. Her iki malzeme de yapısal ve morfolojik olarak karakterize edildi. Argon atmosferinde sentezlenen HEO'nun (HEO-Ar), havada sentezlenene (HEO-Air) kıyasla artan elektrokimyasal performansı gösterilmiştir. HEO-Ar örneğindeki x-ışını fotoelektron spektroskopisi yöntemiyle karakterize edilen oksijen boşlukları, Li+ konaklama bölgelerinin sayısını artırarak, iletkenliği artırarak ve Li+ difüzyon

kinetiğini hızlandırarak elektrokimyasal performansları iyileştirir. Her iki malzeme de daha yüksek özgül kapasiteye sahip olmalarına rağmen, grafit ile karşılaştırıldığında daha yüksek çalışma voltajı sergilerler. Bu özellikleri bilmek, hem malzeme tasarımcısına hem de hücre tasarımcısına, enerji depolamanın spesifik uygulamasına göre malzemeleri ve elektrokimyasal hücreleri tasarlama yeteneği verir. Geliştirilmiş akım hızı yetenekleri ve uzatılmış çevrim ömürleri göz önüne alındığında, bu malzemelerin muhtemelen pik tıraşlama, şebeke desteği ve yenilenebilir enerji depolama gibi şebeke düzeyindeki uygulamalarda kullanılması mümkündür.

Anahtar Kelimeler: Lityum-İyon Bataryalar, Yüksek Entropili Oksitler, Anotlar

To my family,

ACKNOWLEDGMENTS

I would like to extend my sincere gratitude to my mentor Dr. Çiğdem Toparlı for all her assistance with the research, including advice, criticism, support, and insight.

I am grateful to Dr. Ersu Lökçü, my co-advisor, for their constant support, mentoring, assistance with and insightful advice.

I owe a debt of gratitude to Middle East Technical University's professors and staff as well, whose commitment to academic quality has fostered an atmosphere that is favorable to both learning and research.

I'm grateful to my fiancé Ece and my family for their never-ending love, support, and inspiration while I've pursued my academic goals. Your confidence in me has served as a continual inspiration.

Last but not least, I would want to thank my friends and colleagues working at the Electrochemical Energy Materials Lab for their moral support, insightful conversations, and the infrequently lighthearted times that gave much-needed respite from my job.

I want to thank you all for sharing at this important moment in my life.

TABLE OF CONTENTS

LIST OF TABLES

TABLES

LIST OF FIGURES

FIGURES

CHAPTER 1

INTRODUCTION

1.1 Electrochemical Energy Storage and Conversion

The intermittent nature of renewable energy sources like solar and wind must be overcome, and this requires energy storage. It offers a way to store extra energy during times of low demand and release it during periods of high need. This guarantees grid stability and reduces resource waste.

One of the ways to utilize this energy more efficiently is electrochemical energy storage. Batteries, such as lithium-ion batteries, are frequently used for portable devices and electric vehicles due to their high energy density, whereas supercapacitors offer rapid charge and discharge rates, making them suitable for power-intensive applications. Such applications are shown in Figure 1-1 and Figure 1-2.

Electrochemical energy storage uses chemical reactions to store and release electrical energy. Batteries' two main forms are batteries and supercapacitors. The electronics and electric car industries have been completely transformed by lithium-ion batteries. Their high energy density, low self-discharge rates, and lightweight construction contribute to their appeal. By creating solid-state electrolytes, research by Goodenough et al. (2009) has increased battery performance while improving cycle life and safety [1].

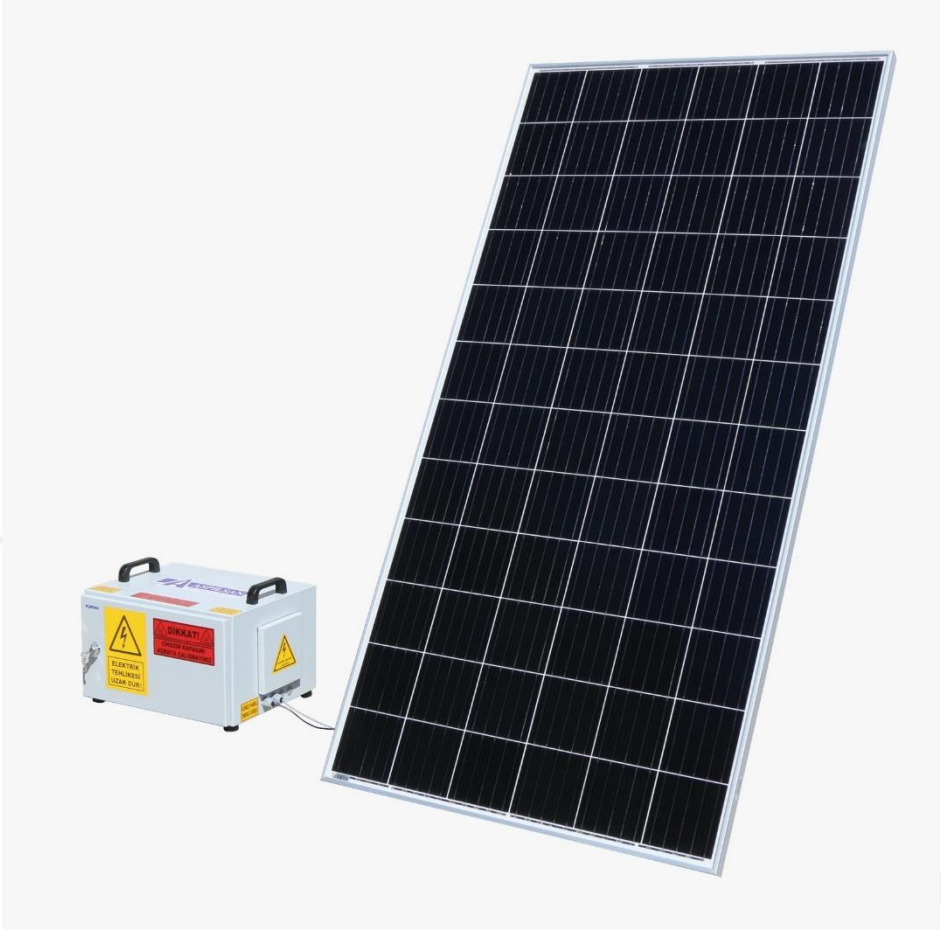

Figure 1-1: Energy storage system coupled with a solar panel [2]

Figure 1-2: Different types of lithium – ion cells produced by Panasonic [3]

Another type of electrochemical energy storage technology that uses liquid electrolytes kept in external tanks are flow batteries. Because of this design's ability to independently scale power and energy capacity, they can be used for grid-level applications. The potential of vanadium redox flow batteries for large-scale energy storage is covered in a paper by Weber et al. (2011) [4].

In contrast to chemical processes, supercapacitors, often referred to as ultracapacitors, store energy by electrostatic charge. Compared to batteries, they have a better power density and longer cycle life. Pandolfo and Hollenkamp (2006) conducted research on the developments and difficulties of supercapacitor technology [5].

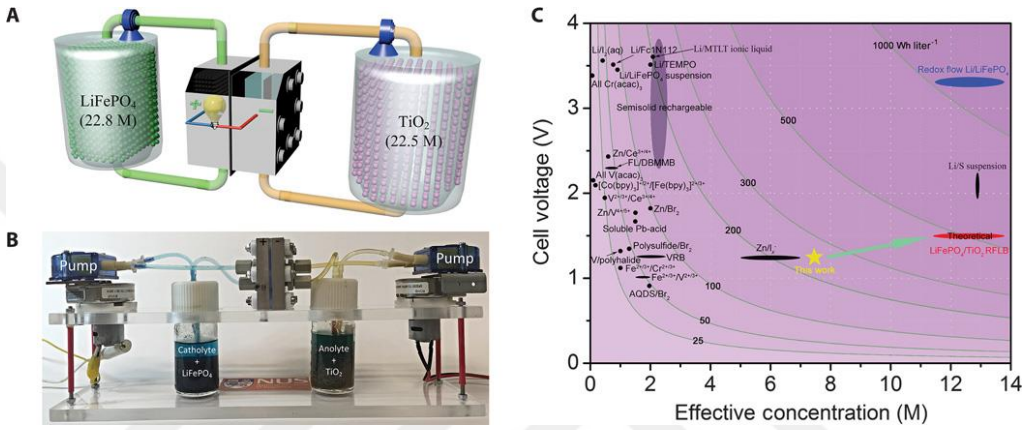

Figure 1-3: Redox flow battery experimental setup and results comparison with literature [6]

Another method that should be mentioned is fuel cell. The only byproduct of hydrogen fuel cells' electrochemical conversion of hydrogen gas into energy and heat is water. These cells have a lot of potential for use in transportation and long-term energy storage. Recent developments in hydrogen fuel cell technology and how they work with renewable energy sources are examined in a review by Kumar et al. (2018) [7].

Figure 1-4: Toyota Mirai showcasing its fuel cell [8]

Due to the costly nature of new infrastructure, the idea of using existing infrastructure has become more and more sought after. One such idea is that Power-to-gas concept. Power-to-gas is a novel energy conversion technique that transforms excess power into synthetic natural gas or hydrogen. The infrastructure already in place may be used to store and transport the generated gas. The viability and promise of power-to-gas technologies for extensive energy storage are examined in research by Götz et al. (2018) [9].

However, most of these methods mentioned are not yet capable of supporting grid-scale energy storage needs. Grid-scale energy storage technologies like compressed air and pumped hydro storage help to keep the electrical grid stable. High capacity and long discharge durations are features of these technologies. Insights into various grid-scale energy storage technologies and their function in energy management are provided by Zakeri and Syri's (2015) research [10].

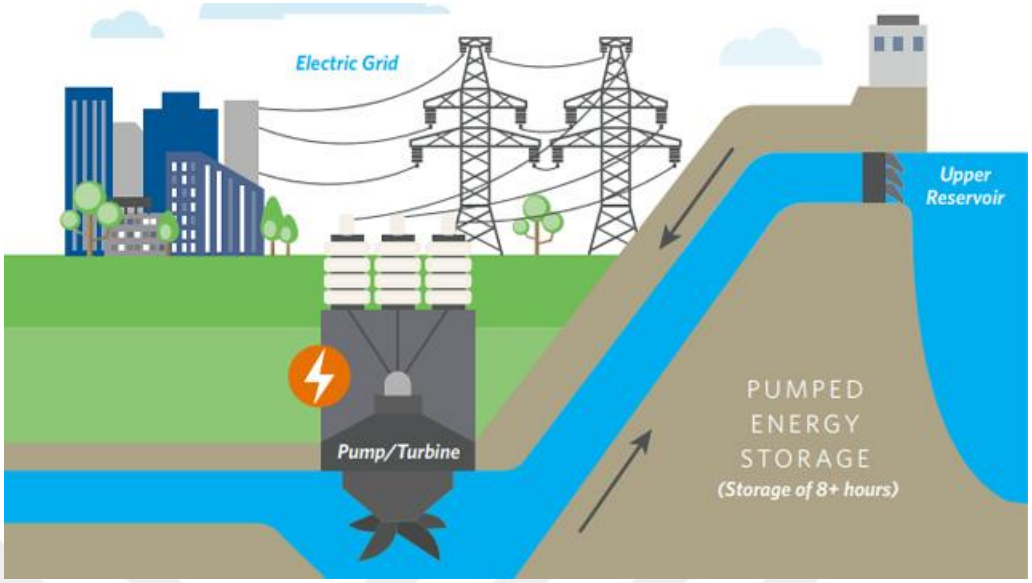

Figure 1-5:Pumped hydro energy storage system schematic [11]

Energy storage and conversion technologies must become increasingly more effective as the need for renewable energy integration rises. Sustainable and reliable energy systems will be made possible by ongoing work on electrochemical energy storage as well as improvements in materials and production techniques.

Batteries, supercapacitors, and hydrogen fuel cells are just a few examples of the electrochemical energy storage devices that are essential for supplying the world's energy needs while facilitating the switch to clean and renewable energy sources. These technologies provide a viable route toward a sustainable and decarbonized future when combined with grid-scale storage options.

1.2 Electrochemical Energy Storage via Lithium – Ion Batteries

Energy production has always been one of the biggest hurdles in the front of the progress of humankind. With the ever-growing need for energy and raising concerns about the environment other methods of energy production have been gaining attention other than fossil fuel – based ones, such as photovoltaic systems and wind

turbines. Energy output of these non-conventional energy producers depends on the meteorological phenomena occurring at the site of installation. However, energy demand and supply aren't always the same and there could always be deficit of the supply. As a remedy to this problem the energy produced by these apparatuses is stored when there is a surplus for later use in the grid.

The methods for energy storage vary by application and other constraints. For large scale stationary systems one of the most widely used methods is pumped hydroelectric storage, where a body of water is pumped into a reservoir at a higher altitude than the original location. But this method has certain geological requirements and at the same time financially burdening which not every nation can overcome on their own. Lately with the increasing installation of renewable energy sources the search for further methods of energy storage is researched. Lithium – ion batteries provide storage at a relative ease compared to their other electrochemical counterparts thanks to their higher specific energy properties. However, the demand for and requirements for batteries have been continually rising. To keep up with requirements of grid level applications, batteries need to be able to respond to frequent surges and sudden high-C charge and discharge phases.

1.2.1 Anode Materials Used in Lithium – Ion Batteries

The performance and general effectiveness of lithium-ion batteries, which are frequently found in various portable electronic gadgets and electric vehicles, are greatly influenced by the anode materials. During the charging and discharging cycles, the anode is the electrode in charge of storing and releasing lithium ions. Researchers have thoroughly investigated a number of anode materials to guarantee high energy density, extended cycle life, and safety. Due to its steady intercalation qualities, graphite has historically been the anode material of choice among these. However, innovative anode materials with increased lithium-ion storage capacity

and stability have been the subject of intense study to address the rising need for higher energy density and quicker charging capabilities.

Graphite, a typical anode material for lithium-ion batteries with a low voltage profile and a theoretical specific capacity of 372 mAh/g. Unfortunately, the cell's impedance increases with cycle count due to the challenging solid-electrolyte interface formation process, leading to subpar performance.

A possible alternative to graphite in lithium-ion batteries is silicon-based anode material. Due to its propensity to alloy with lithium, silicon can theoretically store significantly more lithium ions than graphite. However, during lithiation, silicon expands significantly, which causes pulverization and capacity decline. Researchers have created a variety of silicon nanostructured materials, including silicon nanowires, nanotubes, and nanoparticles, to get around this constraint by reducing the mechanical stress during lithiation. In addition, composite materials that combine the high capacity of silicon with the mechanical durability of carbonaceous materials, such as silicon-carbon nanocomposites, have demonstrated better electrochemical performance [12,13]. Amprius Technologies have recently developed a commercially available cell which can reach up to 450 Wh/kg energy density, using their proprietary anode production method. This method can reach these energy density figures thanks to the usage of silicon nanowires [14].

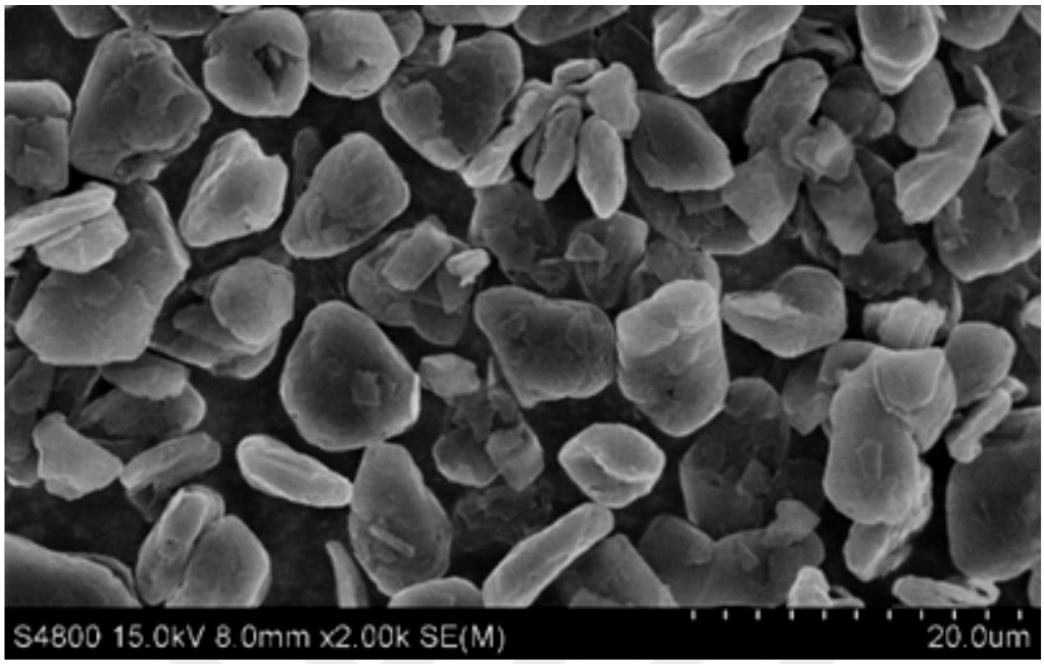

Figure 1-6 BTR New Material Group AGP-7 graphite [15]

As anode materials for lithium-ion batteries, transition metal oxides including tin dioxide (SnO_2), titanium dioxide (TiO_2), and molybdenum trioxide (MoO_3) have also been researched. These substances have high specific capacities and can engage in conversion processes with lithium, which greatly boosts capacity. However, transition metal oxides have significant volume changes during lithiation, which significantly impacts their cycle stability, much like silicon does. Researchers have used nanoscale engineering and the addition of conductive carbon matrices to increase the structural stability of batteries and boost their overall performance in order to overcome this problem [12].

The application of lithium metal anode is another exciting area for lithium-ion battery development. Lithium metal is a desirable material for boosting energy density because of its extraordinarily high theoretical capacity (3862 mAh/g) and low electrochemical potential. However, dendrite growth during cycling has been a problem for lithium metal anodes, which can result in internal short circuits and safety hazards. In order to stabilize the lithium metal interface and reduce dendrite growth, recent research has concentrated on creating artificial solid electrolyte

interphase (SEI) layers and using a variety of electrolyte additives [16]. This has improved the cycling performance and safety of lithium metal anodes in lithium-ion batteries.

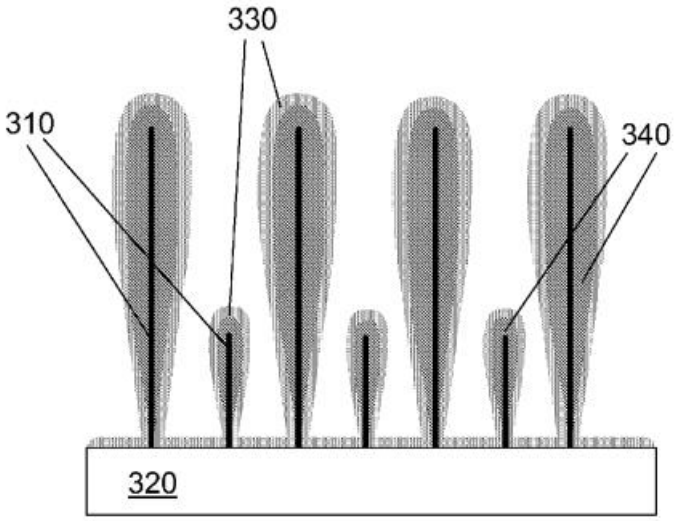

Figure 1-7: Silicon deposition onto nanowires schematic [14]

In conclusion, anode materials have a big impact on how lithium-ion batteries operate and behave. The typical anode material is still graphite, but research is also being done on silicon-based anodes, transition metal oxides, and even lithium metal anodes to attain better energy densities and quicker charging rates. In order for these advanced anode materials to be successful, it is crucial to solve problems with volume growth, cycle stability, and security issues. Realizing the full potential of these anode materials will advance the creation of next-generation lithium-ion batteries and will need continued work in material design, nanoscale engineering, and electrolyte optimization.

1.2.2 Cathode Materials Used in Lithium – Ion Batteries

Lithium-ion batteries properties depend heavily on the performance and efficiency of the cathode materials. During charge and discharge cycles, the cathode, the battery's positive electrode, is in charge of storing and releasing lithium ions. Researchers have been investigating numerous cathode materials with special features to obtain increased energy density, longer cycle life, and improved safety.

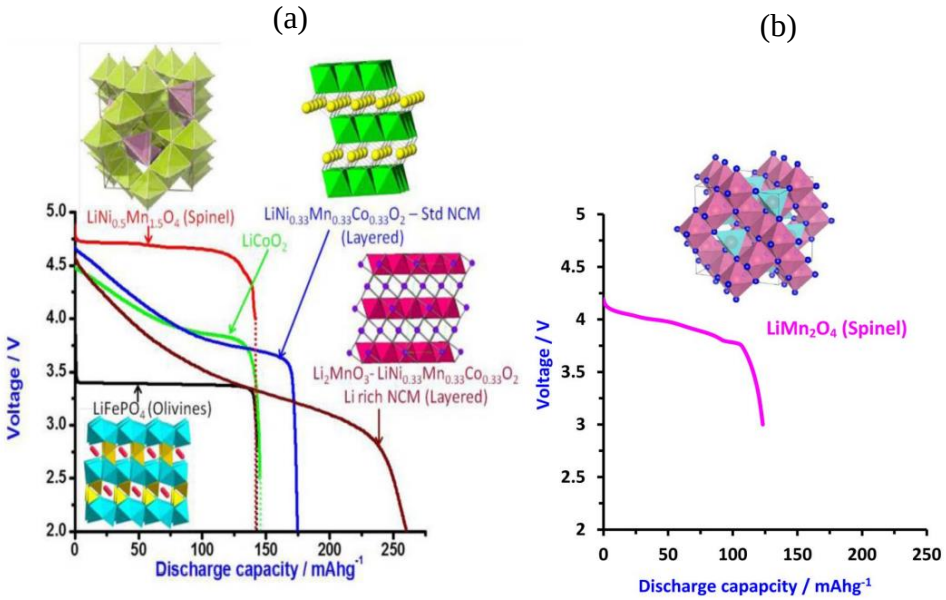

Figure 1-8: Basic equations, architectures, and voltage profiles for lithium-ion battery cathodes. Compared to Li reference electrodes, the potentials are given (a) and (b) [17]

One of the first and most frequently used cathode materials in industrial lithium-ion batteries is lithium cobalt oxide ($LiCoO_2$). It performs well at room temperature and has a high energy density. However, $LiCoO_2$'s instability at high temperatures and vulnerability to thermal runaway raise safety issues, restricting its use in high-power devices and electric cars [18].

Another important cathode material is lithium iron phosphate ($LiFePO_4$), which is renowned for its superior thermal stability and safety features. Compared to $LiCoO_2$, it has a lower energy density, but makes up for it with longer cycle times and a lesser

danger of thermal runaway. $LiFePO_4$ is advantageous for power tools, energy storage devices, and electric buses. Its comparatively poor ionic conductivity, however, might result in rate limitations, which could make it difficult to utilize in high-power applications [19].

A ternary cathode material called Nickel Cobalt Manganese Oxide (NCM) provides a well-balanced mix of high energy density and enhanced thermal stability. NCM cathodes are available in a variety of compositions, such as NCM111 or NCM532, allowing for customization of the performance characteristics of the battery. Electric cars make substantial use of NCM cathodes because of their capacity and power delivery capabilities. Still, more study into cobalt-free solutions has been motivated by the expense and safety issues related to the usage of cobalt [20].

Another common ternary cathode material used in high-performance lithium-ion batteries, notably in electric cars, is lithium nickel cobalt aluminum oxide (NCA). Thanks to the addition of aluminum, which raises the material's overall stability, NCA cathodes are able to offer energy densities that are even greater than those of NCM cathodes. Because of its superior specific capacity and high-rate capabilities, NCA batteries are appropriate for demanding applications. Similar to NCM, the price and scarcity of cobalt continue to be obstacles to its wider use. To meet these problems, efforts are being made to improve the NCA composition and look at cobalt-free options [21].

Future cathode materials for lithium-ion batteries are anticipated to be influenced by a number of significant trends and advancements that aim to enhance performance, safety, and sustainability.

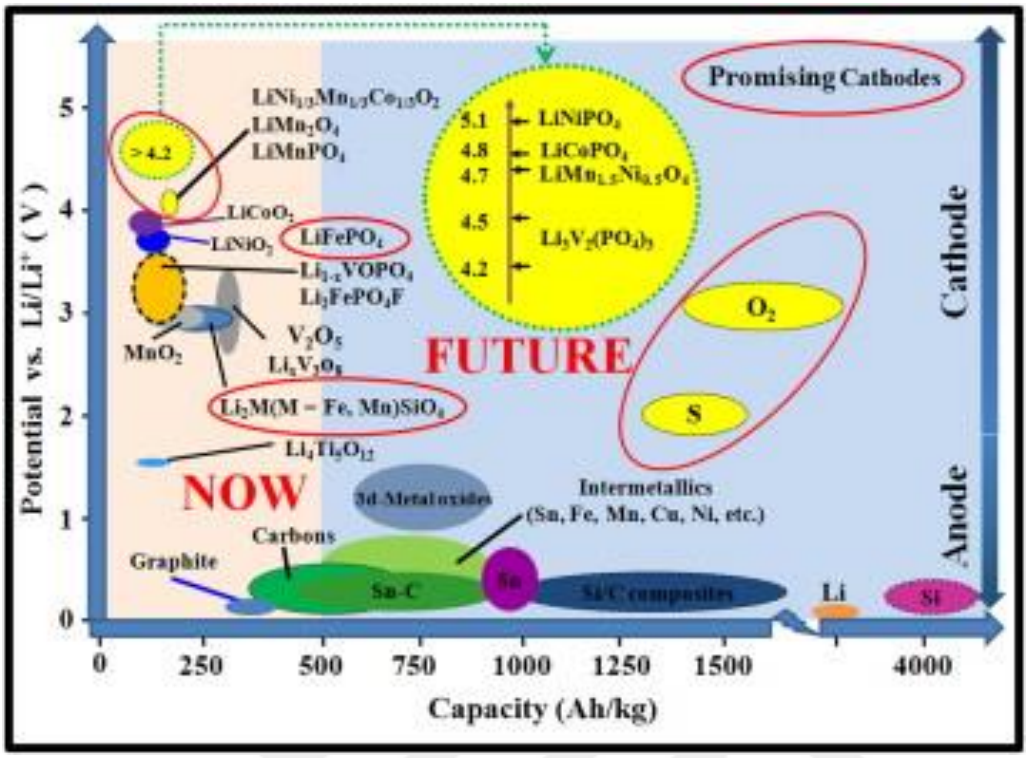

Figure 1-9:Comparative figure of active materials and their corresponding electrochemical performances [22]

1.2.3 Separator Materials Used in Lithium Ion Batteries

The separator material is one essential part of lithium-ion batteries; it is essential for preventing internal short circuits and improving overall battery performance.

To avoid direct contact and the potential for internal short circuits, separator materials used in lithium-ion batteries are generally porous membranes positioned between the positive and negative electrodes. Specific qualities including strong ionic conductivity, mechanical strength, thermal stability, and chemical resistance should be present in these separators. Due to their good thermal stability and affordable production, polyolefin-based separators are the most popular option in commercial lithium-ion batteries [23]. Usually constructed of polyethylene or polypropylene, these separators have been designed to deliver dependable and constant functioning.

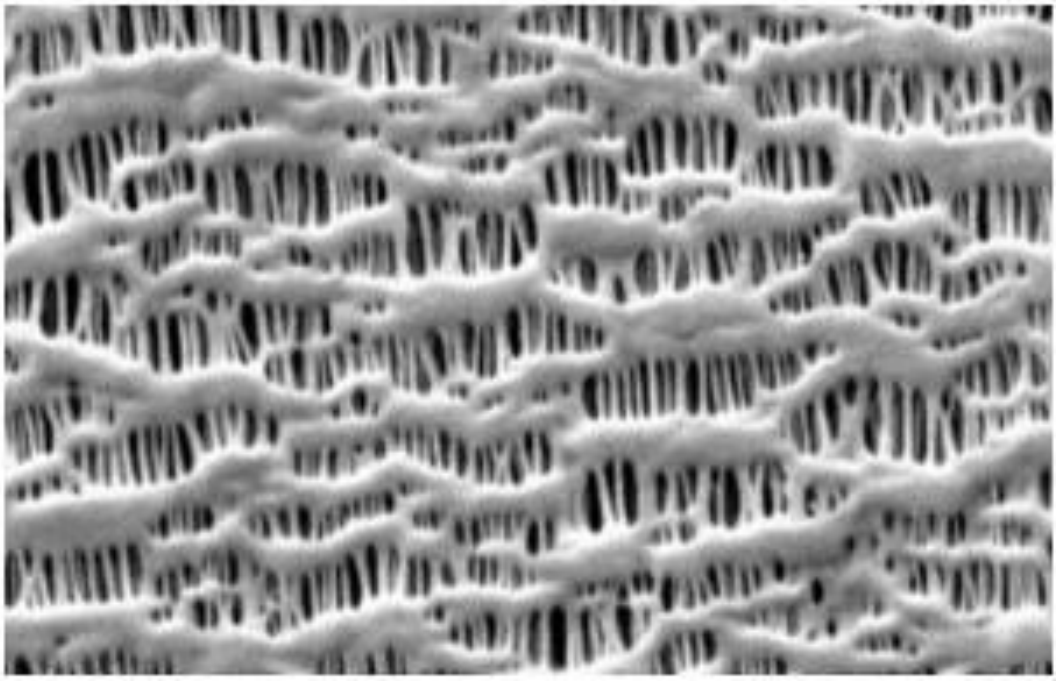

Figure 1-10: SEM image of Celgard 2400 25µm Polypropylene Separator [24]

To enhance battery performance, new separator materials are constantly being investigated. Separators that are coated with ceramic are one such promising material. To improve thermal stability and lower the chance of thermal runaway in lithium-ion batteries, researchers have created ceramic-coated separators [25]. The ceramic coating serves as a physical barrier that can stop the spread of internal short circuits, enhancing the security and dependability of the battery.

Additionally, polymer-based nanocomposite separators have been investigated by researchers. To increase their mechanical strength and heat resistance, these separators have nanoparticles incorporated into them. Incorporating silica nanoparticles into polyethylene separators is another strategy to increase the material's mechanical integrity and thermal stability [26].

Additionally, solid-state electrolytes are a potential replacement for conventional liquid electrolytes in lithium-ion batteries. Solid-state electrolytes are a possible option since they provide improved safety and greater energy density. In contrast to

liquid electrolyte-based batteries, the use of a sulfide-based solid-state electrolyte as the separator and electrolyte in a lithium-ion battery, displaying enhanced safety and performance [27].

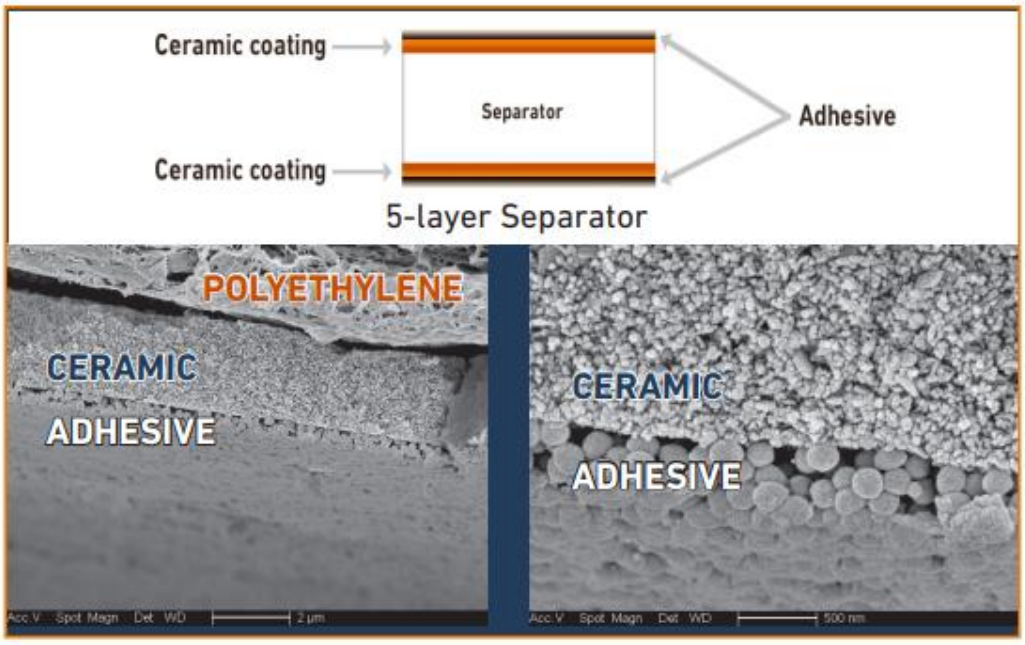

Figure 1-11: Schematic and SEM image of cross section of ceramic coated separator of Entek Membranes LLC [28]

To summarize, separator materials play a crucial role in the safety and overall performance of lithium-ion batteries. To increase battery safety, energy density, and cycle life, current research focuses on enhancing separator materials, such as ceramic-coated separators, nanocomposite separators, and solid-state electrolytes. These developments are essential in the continuous attempt to create lithium-ion battery technologies that are more effective and dependable.

1.2.4 Electrolytes Used in Lithium – Ion Batteries

Electrolytes are essential to the operation of lithium ion batteries because they help transfer lithium ions between the cathode and anode electrodes during charging and discharging cycles. Lithium salts and additives commonly make up these

electrolytes, which are then dissolved in organic solvents to provide a conductive media that facilitates ionic transport. Among other lithium salts, lithium bis(trifluoromethanesulfonyl)imide (LiTFSI), lithium perchlorate ($LiClO_4$), and lithium hexafluorophosphate ($LiPF_6$) are often utilized. Electrolyte selection is also important for the reason that its components are primary components that will form the solid electrolyte interface (SEI). Organic solvents and additives that will be reduced during the first charge of the full cell will form the SEI layer over the anode and will perform as a protective layer against further side reactions.

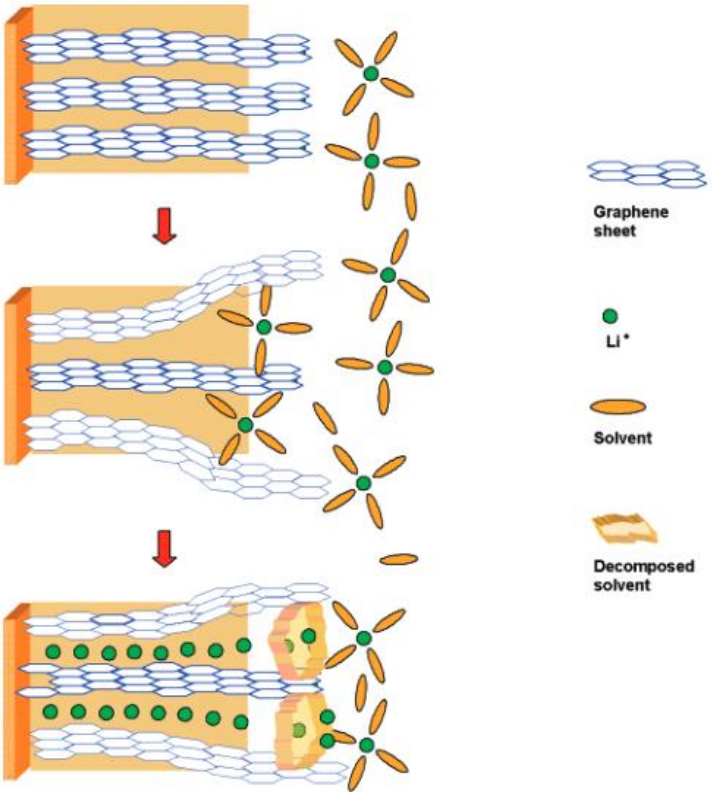

Figure 1-12: SEI layer formation process schematic [29]

Lithium-ion batteries need to use the right electrolytes to provide the required performance, safety, and lifespan. The performance of the battery as a whole is substantially influenced by the composition of the lithium salt and solvent. For instance, LiPF6 is frequently employed because of its high conductivity, but it might compromise safety by causing the creation of dangerous fluorine compounds, such

as hydrofluoric acid, following battery misuse or failure. Alternative lithium salts have been investigated by researchers, such as LiTFSI, which exhibits superior thermal properties and a reduced likelihood of fluorine-related problems [30]. However, LiTFSI is known to facilitate aluminum corrosion ~3.80 V vs. Li/Li^+ [31]. Therefore, when choosing these lithiated salts proper investigation of materials and their interactions are of utmost importance.

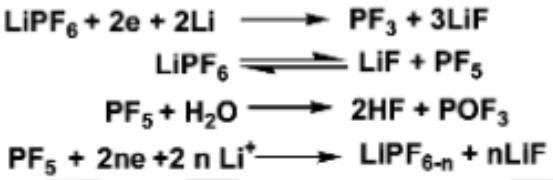

(Equation 1: Dissociation of $LiPF_6$) [30]

The selection of solvents is a crucial factor in the creation of electrolytes for lithium-ion batteries. Because they work well with ordinary lithium salts, conventional carbonate-based solvents like ethylene carbonate (EC), dimethyl carbonate (DMC) and diethyl carbonate (DEC) are frequently utilized. They have a constrained voltage stability, though, which can result in electrolyte breakdown and eventually shorter battery life. To increase voltage stability and boost battery performance, researchers have been striving to include innovative solvents, such as fluorinated solvents or ionic liquids [30].

Particularly ionic liquids have attracted interest because to their special characteristics, including low volatility, non-flammability, and broad electrochemical stability windows. Compared to conventional organic solvents, they may provide greater safety and performance. Before they are widely used in commerce, nevertheless, issues with their high cost and high viscosity still need to be resolved [32].

Innovations in lithium-ion battery electrolytes are being made with a focus on sustainability as well as increasing the performance and safety of these batteries. To replace conventional non-renewable lithium salts and organic solvents, researchers

are looking towards greener, more ecologically friendly electrolytes. To lessen the ecological impact of lithium-ion batteries, novel electrolyte formulations utilizing biomass-derived materials and ecologically friendly lithium salts are being investigated [33].

The performance, safety, and environmental effect of lithium-ion batteries are all influenced by the electrolytes, which constitute a key component of these batteries. The voltage stability, ionic conductivity, and thermal properties of the battery are directly influenced by the choice of lithium salts and solvents. Research is being done to create electrolytes that not only improve the performance and safety of lithium-ion batteries but also adhere to the fundamentals of environmental responsibility as technology develops and sustainability becomes a bigger issue.

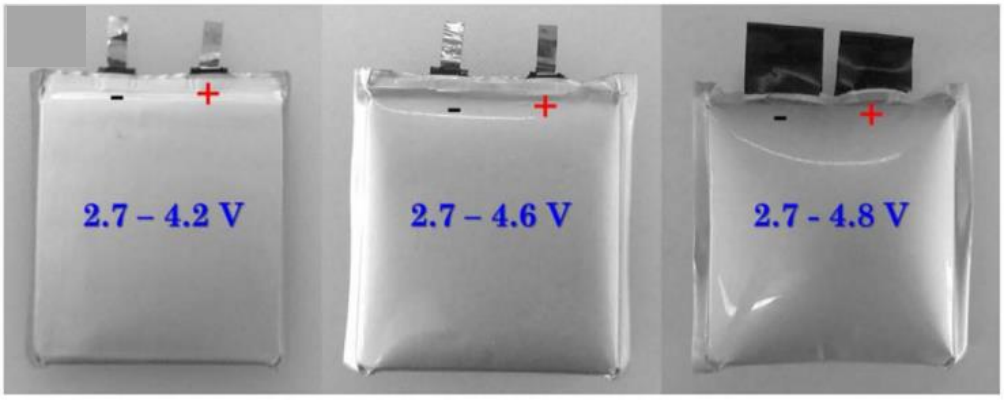

Figure 1-13: Gassing induced volume expansion of the cells cycled using different cutoff voltages [34]

To increase the performance of batteries, several methods and materials are being researched, such as alloying and conversion type materials. The transition metal oxides (TMOs) have been the subject of in-depth research. Nevertheless, because of the significant volume shift that occurs during lithiation and delithiation, materials have shown short cycle life and stability. Another family of recently found materials is high entropy oxides (HEO). The initial research on high entropy materials was done by Yeh (2004) and Cantor (2004) [35,36]. Many high entropy materials,

including alloys, oxides, carbides, nitrides, and others, have been researched over time [37-42]. According to the idea of high entropy materials, material properties may be changed by varying compositions. It is recognized practice that a substance must have configurational entropy more than 1.5 R (R, universal gas constant) in order to be categorized as a "high entropy" substance [42].

HEOs with rock-salt and spinel structures have recently become the subject of study [43-46]. Solid-state synthesis, nebulized spray pyrolysis, solgel, and co-precipitation are just a few of the production methods that have been employed. Compared to HEOs made with four cations, those made with five cations have demonstrated more consistent performance [41].

Yet, this category of materials also has drawbacks. The World Bank predicts that commodities prices will climb further. The adoption of this type of material will be impacted by the price increases and fluctuations of the commodities market because battery grade graphites cost just a few dollars per kilogram compared to the market pricing for nickel and copper, which are respectively 25,000 and 9,000 dollars per ton [47]. The majority of the research materials found in the literature have a high price tag, including cobalt, copper, nickel, zinc, and titanium. The fact that HEOs have higher voltage values vs. Li/Li^+ than graphite is another drawback [48] of HEO technology.

1.3 Aim of This Study

HEOs provide several possible advantageous traits compared to the contemporary active materials used for electrochemical energy storage. One of them is due to the nature of the materials their properties are tunable. These materials can be designed specifically to satisfy the needs of application via changing the composition and stoichiometry of the components.

HEOs show enhanced properties in terms of capacity, rate capability and capacity retention both in this work and in the literature. These enhancements in turn may enable better performance in real-life applications.

The primary objective of this study is to investigate and discuss the properties of high entropy oxide materials in lithium-ion batteries as anode material. For this reason, starting with the initial composition of $(Fe_{0.2}\ Cr_{0.2}\ Co_{0.2}\ Mn_{0.2}\ Zn_{0.2})_3O_4$ various single-phase materials were synthesized, electrochemically, morphologically, and structurally characterized. It is believed that as research on HEOs continue their real-life applications may come to realization.

CHAPTER 2

LITERATURE REVIEW

2.1 High Entropy Materials

Since ancient times of humankind civilizations have been working with metals and have been modifying them in accordance with their needs. Up until recent years metal working and alloying was done around primary elements constituting a major part of the alloy and secondary elements constituting minor fraction of the said alloys. With this approach the number of variations produced is limited. Another approach is based around mixing multiple primary elements with equimolar proportions. This approach has opened the road for research in many fields. These materials were then called high-entropy materials because of their high entropy nature [49].

Due to their distinct structural features and extraordinary properties, high entropy materials (HEMs) are a potential class of advanced materials that have attracted a lot of interest recently. HEMs have a highly disordered atomic structure because they are made up of many elements in about equal amounts, as opposed to normal alloys, which generally include one or two core elements. The high entropy produced by this compositional complexity is thought to improve the materials' mechanical, thermal, and magnetic characteristics.

Yeh and Cantor (2004) conducted the first studies on high entropy materials [35, 36]. These new classes of materials have been studied in several domains, including energy storage, catalysis, dielectric, magnetic, and optical applications, ever since the first high entropy materials were described. The concept of high entropy

materials states that different compositions can alter the qualities of a material. According to accepted practice, a material qualifies as "high entropy" if its configurational entropy exceeds 1.5 R (R, the universal gas constant) [42]. Calculation of change of configurational entropy for equimolar solid solution composed of n elements is done via following equation.

$$\Delta S_{conf} = -k \ln (w) \quad \text{(Equation 2)}$$

$$\Delta S_{conf} = -R(1/n\, ln\, 1/n + \ 1/n\, ln\, 1/n + \cdots 1/n\, ln\, 1/n) \quad \text{(Equation 3)}$$

$$\Delta S_{conf} = -Rln\frac{1}{n} = R \ln(n) \quad \text{(Equation 4)}$$

Where k is denoted as Boltzmann's constant, w is referred to as the variety of combinations. As it is understood from the equation when number of elements, n, increases configurational entropy increases. It is this principle that created the notion that with high enough entropy, enthalpy of mixing penalty could be overcome, and material becomes stabilized [35, 49].

High entropy materials have remarkable mechanical qualities, which is one of their main benefits. Due to the high level of structural disorder, which precludes the production of big grains, these materials have exceptional mechanical strength and hardness and are inherently resistant to failures caused by failures at the grain boundaries. HEMs are appealing for high-temperature applications since studies have demonstrated that they can retain their strength even at high temperatures. For instance, because of their extraordinary thermal stability, alloy systems like CrMnFeCoNi have been researched for their possible usage in gas turbine engine components [50].

High entropy materials are extremely promising, however there are still issues with their development and scalability. To obtain the desired qualities, careful control over the composition and processing conditions is necessary throughout the design and synthesis of these complex alloys. Their special characteristics might also make it difficult to comprehend their behavior and forecast how well they will function in

diverse applications. High entropy materials are a fascinating field of study with a bright future because of continuing research and partnerships between materials scientists and engineers that push the frontiers of knowledge and application [51].

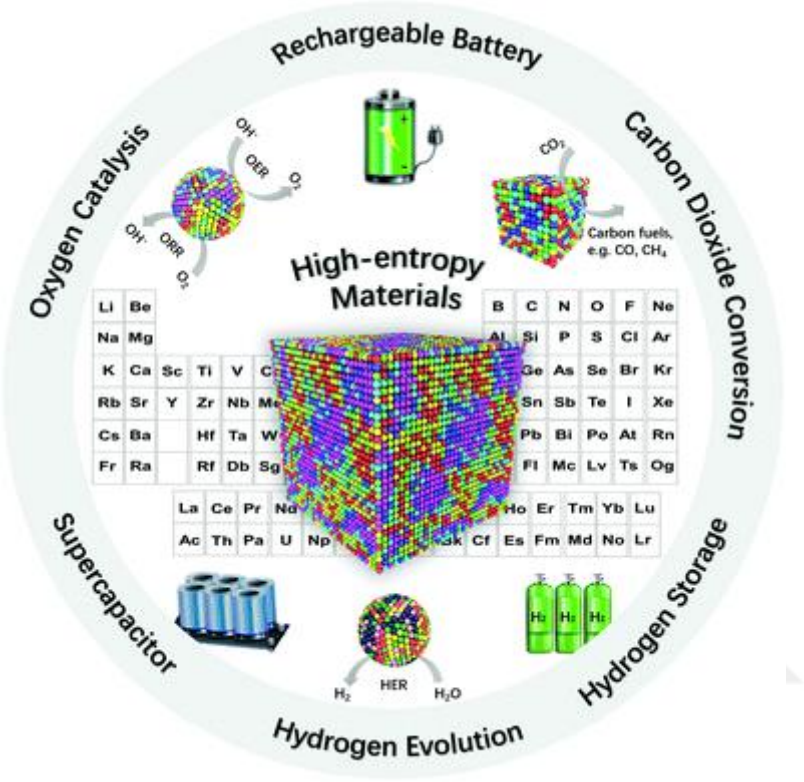

Figure 2-1: A diagram of potential usages of High Entropy Materials [52]

2.2 High Entropy Oxides

High entropy oxides (HEOs) are an intriguing family of materials that have gained a lot of interest recently because of their distinctive characteristics and possible uses. HEOs are made up of numerous metal cations in a disordered arrangement as opposed to traditional binary or ternary oxides, which results in a high degree of structural complexity and high entropy. Because of the new and adaptable functions that this disorder confers, HEOs are interesting candidates for a variety of technological applications.

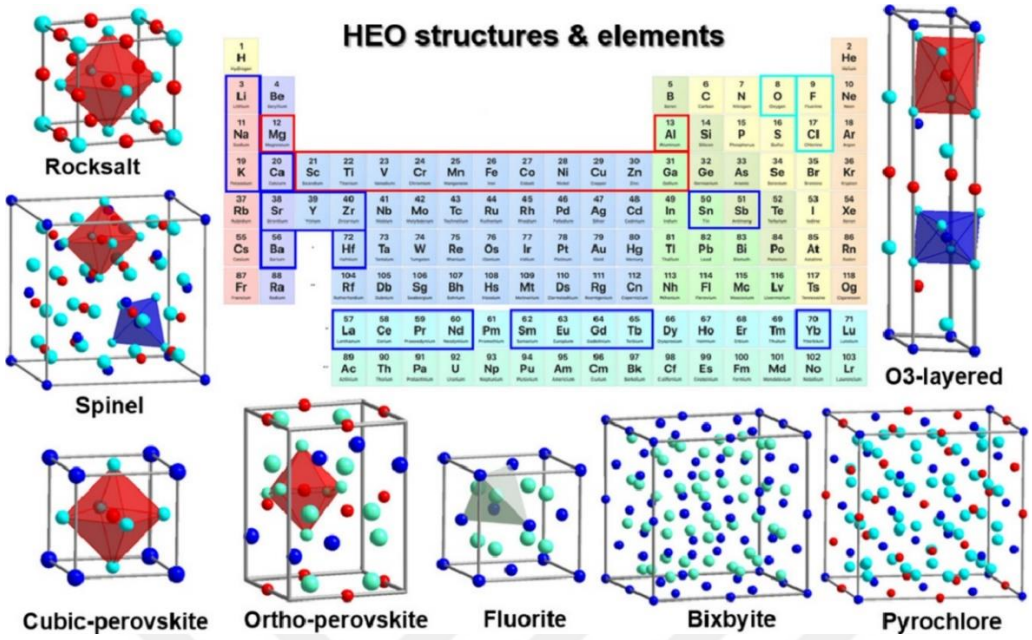

Figure 2-2: Several high entropy oxide material structures being researched for catalysis, electrochemical energy storage, hydrogen evolution [40]

The high configurational entropy of HEOs is responsible for their outstanding thermal stability. HEOs are particularly appealing for high-temperature applications such as catalyst, thermal coatings, and refractory because the random distribution of cations in the lattice minimizes the propensity for grain formation and phase separation. The stability of metastable phases is also made possible by the high entropy composition, expanding the set of capabilities.

The tailorable electrical and optical capabilities of HEOs are one of its key features. Unique electronic structures are produced when many metal cations with various valence states and coordination environments are present in the lattice. Designing new electrical and optoelectronic devices is made possible by this electronic complexity. In order to improve ion transport and electrochemical performance in batteries and fuel cells, researchers have also looked into the potential of HEOs in energy storage and conversion applications.

The extraordinary mechanical characteristics of HEOs, such as their great hardness, strength, and wear resistance, have also been studied. HEOs' chaotic atomic

configuration prevents dislocations from spreading, which increases mechanical stability. Due of these characteristics, HEOs have attracted attention for use in cutting tools, wear-resistant coatings, and other structural applications requiring high mechanical performance.

HEOs have enormous potential, but because of the large amount of compositional space they cover, their design and synthesis remain difficult. In order to forecast and investigate novel HEO compositions, computational approaches, such as first-principles computations and high-throughput screening, are essential. Recent advancements in experimental synthesis and characterization methods have also made it possible to realize high entropy compositions that were not before possible.

For simpler explanation of thermodynamics of high entropy oxides, a system of binary metallic system composed of A and B is given. Interactions energy between these components are given by the following formula:

$$E_{I(A-B)} = \frac{E_{I(A-A)} + E_{I(B-B)}}{2} \quad \text{(Equation 5)}$$

Where it is assumed that ΔH_{mix} is zero then that leads to atoms in the solution contribute with maximum entropy to the system. For all metal oxide structure cations are surrounded by oxygen anions, leading to a separation of cation layers by anion layers. When this phenomenon is considered, cations will be contributing to the lattice equally driving the whole system to its maximum entropy [53].

In the literature it is reported that ionic radii, electronegativity, crystal structure and coordination number of cations should be similar to form a single-phase high entropy oxide system [53, 54].

For the synthesis of this group of materials; solid-state, spark plasma sintering, combustion-based methods, nebulized spray pyrolysis, hydro-thermal and solvo-thermal methods, sol-gel methods and co-precipitation methods were used.

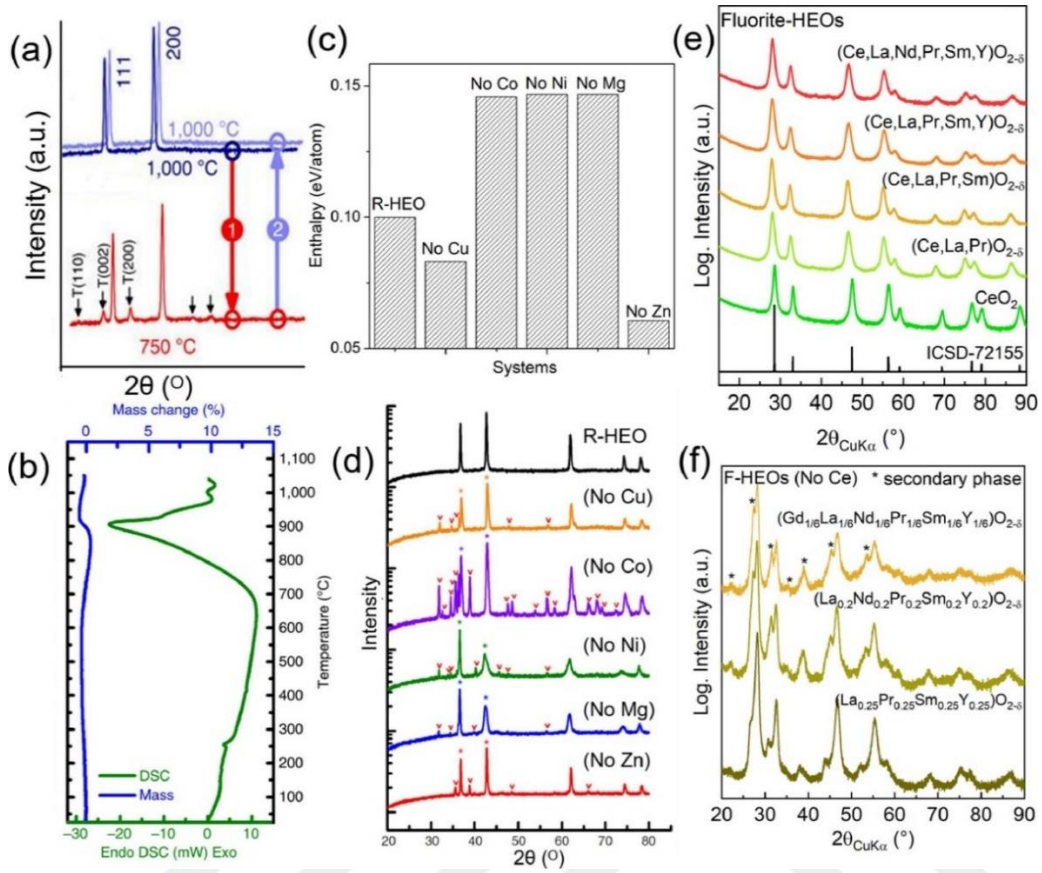

Figure 2-3: Phase transformation and endothermicity of rocksalt HEO is depicted on (a), (b), enthalpic penalty of the systems depending on the cation configuration is computed and plotted on (c), and effect of cations on the HEO structure are depicted on (d) – (f) [40]

High entropy oxide materials are especially researched because of their tailorable properties. In theory one can tailor material specifically to cover their needs. HEO's are thanks to their entropically stabilized structures are believed to have potential uses in electrochemical energy storage, as catalyst, in hydrogen and oxygen evolution reactions, in supercapacitors, hydrogen storage areas [55].

High entropy oxides are a fast-developing scientific topic with a wealth of potential practical applications. They are appealing for a variety of sectors, including electronics, energy storage, and materials engineering, due to their special mix of thermal stability, adjustable characteristics, and superior mechanical performance. We may anticipate future innovations in the creation of these exciting materials as research develops and our knowledge of HEOs increases.

2.3 High Entropy Oxides for Lithium – Ion Storage

Ever since the commercialization of lithium-ion batteries, intercalation type materials, especially graphite, have been the dominant material of choice for anode materials. However, due to their limited specific capacities the progress of lithium-ion battery technology was limited. One type of candidate for new type of lithium-ion batteries are conversion type lithium-ion storing materials. Generally, they are composed of transition metal oxides, sulfides, fluorides, phosphides, and nitrides. These types of materials are considered promising because of their relatively high specific capacities and low cost compared to conventional anode materials used in LIB's. Generally, conversion reactions for lithium-ion storage may be expressed as [56]:

$$X_aY_b + (b\ x\ c)Li^+ + (b\ x\ c)e^- \rightleftarrows aX^0 + bLi_cX \qquad \text{(Equation 6)}$$

Where X denotes cationic and Y anionic species. X may be transition metal or a group of transition metals, Y can be any type of anions mentioned before. When X contains five or more members and Y is oxygen configurational entropy of the material exceeds 1.5 R and it is considered as high entropy oxide material. High entropy oxides due to entropy stabilization of the structure has seen increased research activity. With different combinations of five or more metal cations some of those single-phase materials show interesting properties in terms of cycle life and reversible capacity. High levels of structural disorder brought on by the presence of several metal cations boost entropy and improve the kinetics of lithium-ion diffusion. As mentioned in the previous chapters, since the material properties depend on the type and stoichiometry of the metal cations present, this class of material allows for tailoring of electrochemical properties.

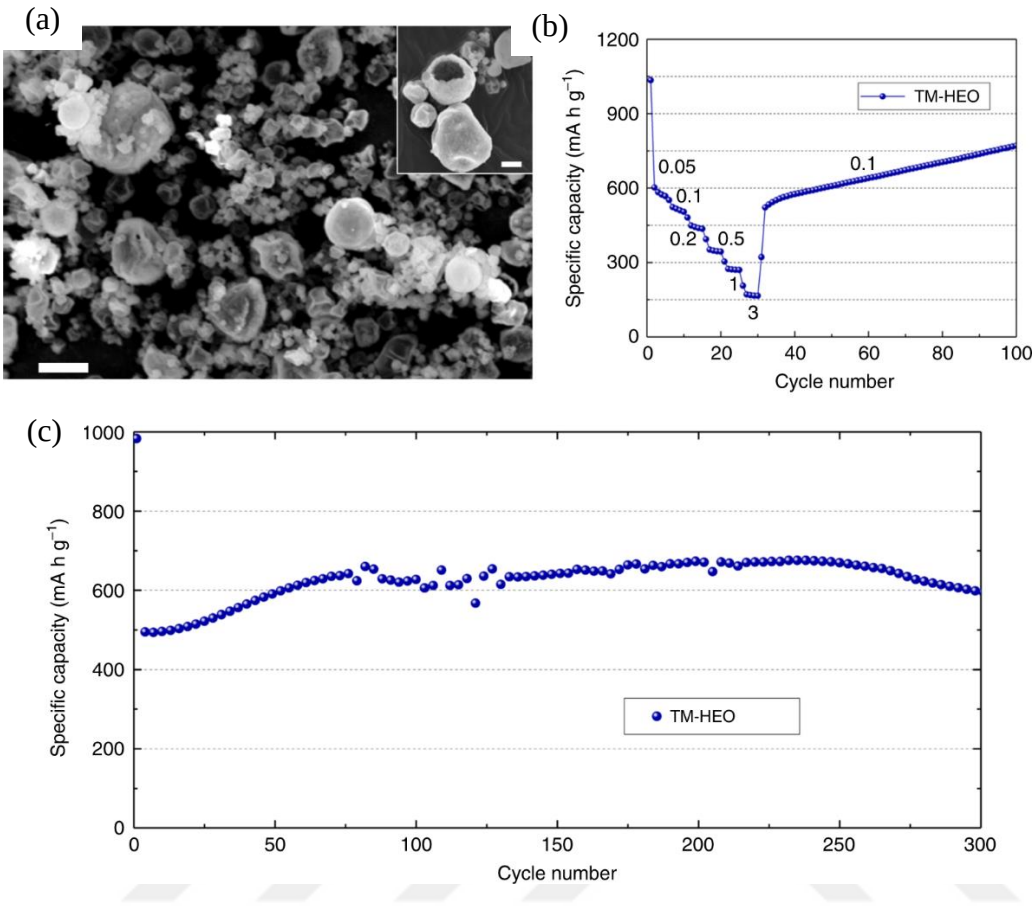

Figure 2-4: HEO material SEM image (a), specific capacity of HEO material under different current rates (b), cycle test of HEO at constant current rate (c) [41]

Lithium-ion storage mechanism for high entropy oxide materials depends on the individual cationic components. Although generally transition metals in the HEO's store lithium-ions via conversion reactions, some of them like zinc store lithium-ions by alloying and some of the elements like magnesium does not go into any reaction and is thought to act as a scaffolding for HEO's [41].

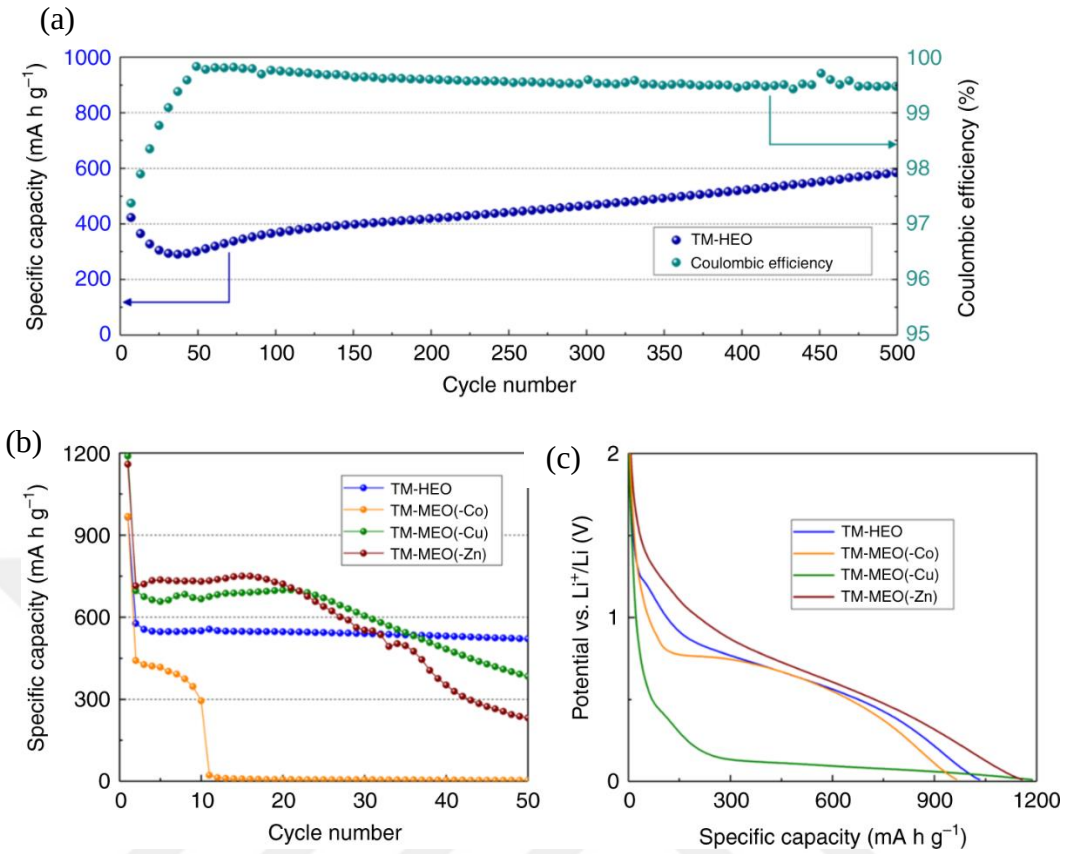

Figure 2-5: Long term cycle and coulombic efficiency test of HEO material (a), effect of cation composition on the electrochemical performance (b), (c) [41]

Although many types of high entropy oxide material have been investigated, most of the work is done on the materials with rock-salt and spinel structures for lithium-ion battery applications [57]. Even though transition metals are chosen as cationic species in the research materials, some of the systems containing elements like Li, Na, K have also been investigated [58, 59].

Even though high entropy oxides hold a lot of potential for lithium-ion storage, issues with their synthesis and scalability must be resolved. Nevertheless, continuous research and development activities keep revealing fresh HEO compositions and enhanced synthesis processes, bringing us one step closer to real-world use in cutting-edge lithium-ion batteries. High entropy oxides have the potential to revolutionize energy storage as the area develops and be a key factor in the shift to a sustainable and effective energy future.

CHAPTER 3

EXPERIMENTAL PROCEDURE

3.1 Material Synthesis

$(FeMnCrCoZn)_3O_4$ powders have been produced using the coprecipitation method. Stoichiometric concentrations of metal nitrate salts were dissolved in DI water and vigorously agitated to produce a homogenous solution. The precipitating agent, aqueous 1 M KOH solution, was then gradually added to the mixture until pH 12.0 was attained. The precipitated particles were then washed and filtered. The resulting powders were filtered and then dried at 110°C for 8 hours. The dried powders were then calcined at 900°C for 90 minutes in an argon and air environment in an atmosphere-controlled tubular furnace. Here, $(FeMnCrCoZn)_3O_4$ powders that were calcined in argon were referred to as HEO-Ar and $(FeMnCrCoZn)_3O_4$ powders that were calcined in air as HEO-Air.

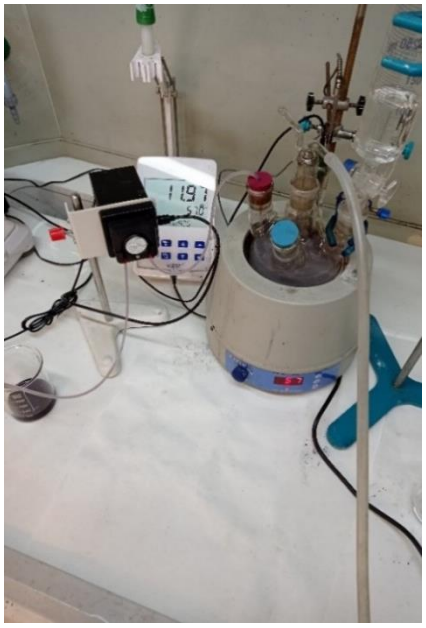

Figure 3-1: Co-precipitation reactor setup

Table 3-1: Materials used in the synthesis and cell preparation

MATERIAL	PRODUCT SOURCE	PURPOSE
$Fe_2(SO_4)_3.H_2O$	Sigma Aldrich 307718	Iron source in HEO
$CoSO_4.7H_2O$	Sigma Aldrich C6768	Cobalt source in HEO
$MnSO_4.H_2O$	Sigma Aldrich M7634	Manganese source in HEO
$Cr(NO_3)_3.9H_2O$	Sigma Aldrich 239259	Chromium source in HEO
$ZnSO_4.7H_2O$	Sigma Aldrich 221376	Zinc source in HEO
KOH	Sigma Aldrich 06103	Precipitating agent
NH_4OH	Sigma Aldrich 105428	Chelating agent
Coin cell assembly kit	Gelon Lib Group	Half-cell testing
PE separator 25 um	Nanografi NG04CO08032	Anode-cathode separation
1.0 m $LiPF_6$ in EC/DEC 50/50 (v/v)	Sigma Aldrich 746746	Electrolyte
Copper foil 10 um	Nanografi NG08BE03011	Current collector
N-methyl-2-pyrrolidone	Nanografi NG04CO08027	Solvent
Poly (vinylidene fluoride)	Nanografi NG08BE1101	Binder
Carbon black	Nanografi NG04CO08029	Conductive additive
Lithium metal	Sigma Aldrich 265985	Counter and reference electrode

3.2 Structural and Morphological Characterizations

Powder X-ray diffraction (XRD, Rigaku) was used to study the crystal structures of the HEO under Cu K radiation (λ = 1.5406 Å). The XRD patterns were refined using the Rietveld Refinement Method and the GSAS software and the EXPGUI interface.

Field emission scanning electron microscopy (SEM, FEI Nova Nano SEM 430) was employed to analyze the morphology and microstructure of the samples.

Using Al Kα radiation and X-ray photoelectron spectroscopy (XPS, PHI 5000 Versa Probe spectrometer), the chemical make-up and condition of the HEO powders were investigated.

3.3 Electrochemical Cell Preparation and Characterizations

Electrodes were assembled by combining 75 weight percent HEO powder, active material, 15 weight percent Carbon Black, used as conductive agent, and 10 weight percent PVDF, used as binder, in NMP solvent. The resulting slurry was applied via a Dr. Blade on Cu foil of 10 μm and overnight vacuum-dried at 80^{o}C. For 12 mm diameter disc-shaped electrodes, the average mass loading of the active materials was estimated to be 1.5 mg. To have a more reproducible result and neglect the effect of different mass loadings in the electrodes, electrodes of active mass loading of 1.5 mg were selected and used in the coin cell assembly. Both the counter electrode and the reference electrode were made of lithium metal. As a separator, polyethylene membrane was employed. 1 M $LiPF_6$ in (EC/DEC) (50/50 vol) used as electrolyte. Materials listed in table 3-1 were used in this process.

During the electrochemical tests working electrode is designated as various high entropy oxides. Counter and reference electrode is designated as lithium metal (2-electrode testing is applied).

The charge-discharge battery experiments were carried out at various current densities in a potential window between 0.01 and 3.00 V (vs Li/Li+).

Using different scan speeds, cyclic voltammetry (CV) curves between 0.01 and 3.0 V (versus Li/Li+) were measured. During CV electrode materials undergo oxidation and reduction reactions, some of which are reversible and some of which irreversible. Current response with respect to applied differential voltage is measured. These current responses, depending on the voltage sweep vector indicate oxidation or reduction. With this method electrode materials activity regions can be observed. In the case of HEO for lithium-ion batteries, CV helps us determine electrochemically active voltage regions and eventually allows us for tailorable voltage profile. CV gives information about diffusion therefore, enabling comparison of material electrochemical performance.

Electrochemical impedance spectroscopy (EIS) measurements used frequency ranges of 0.01 to 10,000 Hz and an amplitude of 5 mV. EIS measurements allows for investigation of different phenomena occurring inside the cell. A very small amplitude sinusoidal disturbance is introduced to the battery cell during the EIS measurement, and the system's frequency-dependent response is then analyzed. This response includes details on phenomena including capacitive behavior, ion diffusion, and charge transfer resistance. This information aids in evaluating elements like electrode materials, electrolyte composition, and cell design that have an impact on overall battery design.

The kinetics of the electrodes' lithium storage were further studied using the galvanostatic intermittent titration technique (GITT) experiments. During GITT experiments constant current pulses intermittently applied to a cell and the voltage responses are observed. It is possible to collect important data regarding several electrochemical characteristics including diffusion kinetics, charge transfer resistances, and ion concentration gradients by applying controlled current pulses and giving enough relaxation time in between.

CHAPTER 4

RESULTS AND DISCUSSIONS

"This chapter contains information used with the permission of JOHN/WILEY & SONS LTD. from "Effect of synthesis environment on the electrochemical properties of $(FeMnCrCoZn)_3O_4$", Deniz Okan Bayraktar, Ersu Lökçü, Tuncay Erdil, Çağla Özgür, Çiğdem Toparlı, International Journal of Energy Research, 46, 2022; permission conveyed through Copyright Clearance Center, Inc."

The XRD patterns of the powders HEO-Ar and HEO-Air are displayed in Figure 4-1. Peak shapes and intensities reveal that the samples have shown a spinel structure with a space group of Fd-3m, which is a sign of good crystallization (ICDD #04-024-0120). Neither HEO-Ar, nor HEO-Air does not show the presence of impurities. On the other hand, it is discovered that the HEO-Ar sample's XRD peaks had a propensity to move at lower 2ɵ degrees. Figure 4-3 makes this change quite evident, and it may be explained by variations in the amount of oxygen vacancies in the samples [60, 61]. The Rietveld Refinement analysis was also carried out to examine how the lattice parameters changed with the synthesis environment.

Table 4-1: Rietveld Refinement data

Material	Lattice Parameter (Å)	Space Group	Unit Volume ($Å^3$)	Rwp (%)
HEO - Ar	8.425	Fd-3m	598.054	34.7
HEO - Air	8.354	Fd-3m	582.982	18.8

The refinement results are shown in Figure 4-1. For the HEO-Ar and HEO-Air samples, the lattice parameters are determined to be 8.425 Å and 8.354 Å, respectively. SEM images of the HEO-Ar and HEO-Air samples are shown in

Figures 4-4 and 4-5, respectively. Particles in both samples have non-homogeneous shapes and are submicron in size, typically between 100 and 200 nm. Additionally, due to the samples' submicron size, some areas see particle agglomeration. Additionally presented for the samples in Figures 4-4 and 4-5 is the EDS mapping analysis. According to the EDX findings, the structure's Fe, Cr, Co, Mn, Zn, and O elements are distributed uniformly throughout at the micrometer scale.

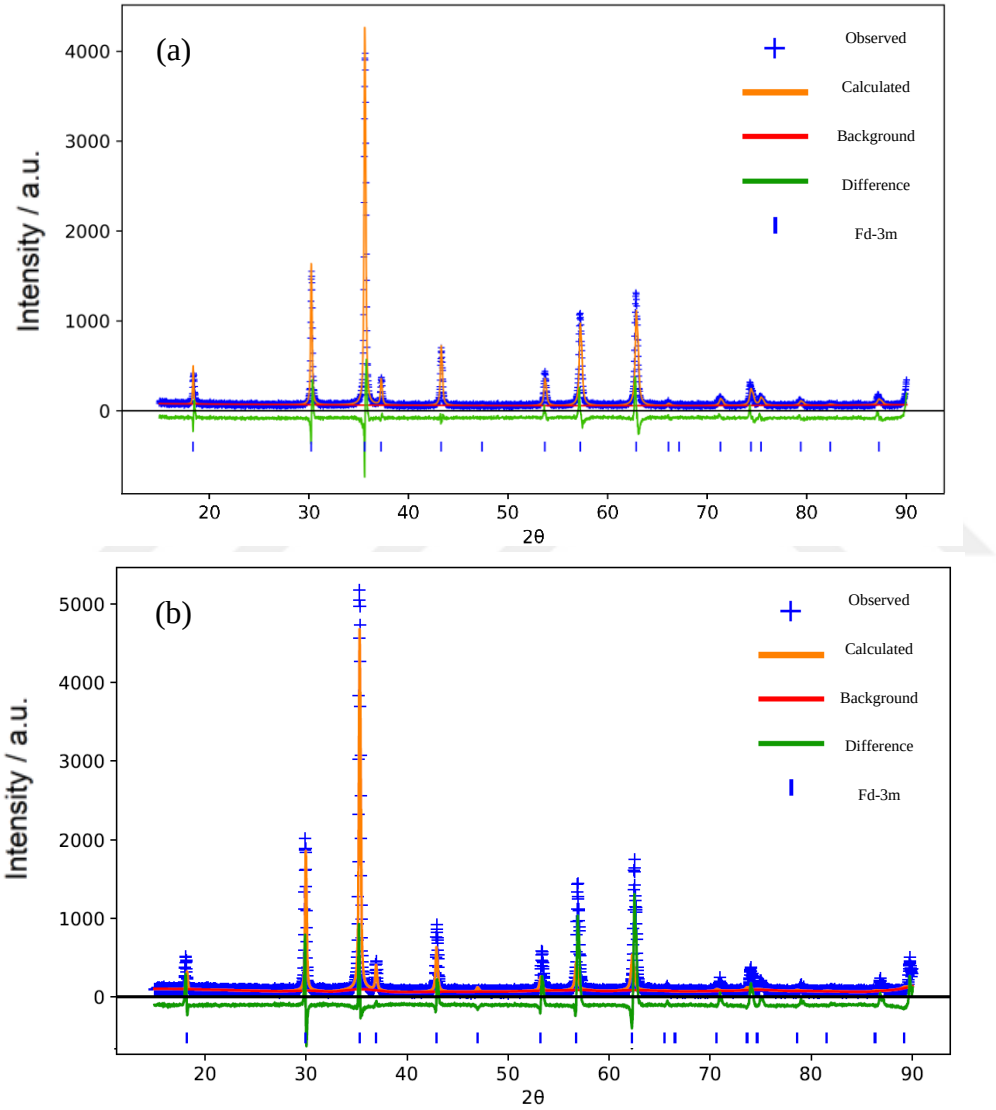

Figure 4-1: Rietveld Refinement Analysis of HEO-Air (a) and HEO-Ar (b)

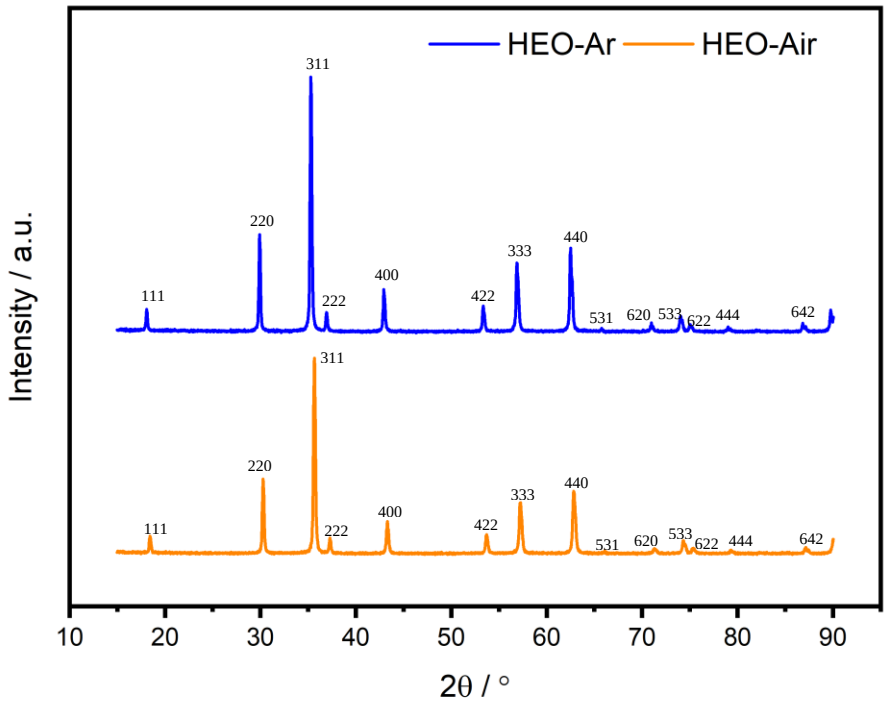

Figure 4-2: X-ray diffraction patterns of HEO-Ar and HEO-Air [77]

In addition to XRD and SEM-EDS examination, the XPS survey spectra of the HEO-Ar and HEO-Air show no impurities are present in the samples. Figure 4-6 displays the peak spectra of samples for Fe, Cr, Co, Mn, and Zn, whereas Figure 4-7 displays the peak spectrum for O. The Fe 2p core level spectra of the samples are shown in Figure 4-6. Deconvolution of the Fe 2p spectra is made challenging by the overlap of the Co LMM and Fe 2p peaks [62, 63]. The Fe $2p_{3/2}$ spectra, however, reveals a particular satellite structure for Fe^{3+}. Therefore, it may be concluded that materials calcined in argon are dominated by Fe^{3+} ions, whereas samples calcined in air are dominated by the Fe^{2+} state. In Figure 4-6, spectra for Mn 2p are shown. It should be noticed that whereas the sample calcined in the Ar environment retains its MnO satellite characteristic, the sample calcined in the air does not. The air-calcined sample contains MnO, according to the XPS results, whereas the other samples have Mn_2O_3.

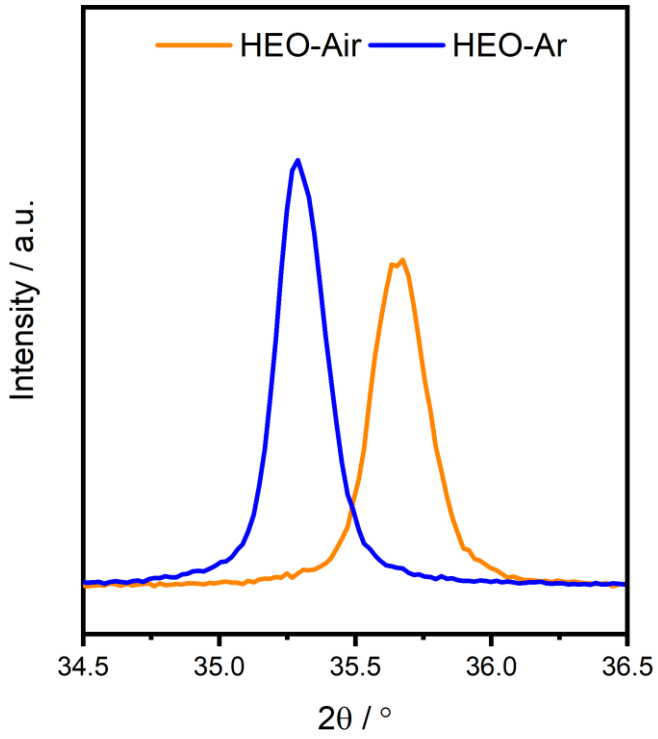

Figure 4-3: X-ray diffraction patterns of HEO-Ar and HEO-Air, shift in main peak is observed due to changes in structural parameters [77]

The prominent satellite of Co+2 in the Co 2p spectra in Figure 4-6 highlights the fact that Co+2 predominates in all samples [60, 64]. The Zn $2p_{3/2}$ at 1021.3 eV in Figure 3D indicates Zn^{2+} [60]. The Cr+3 state is shown by the peak in the Cr 2p spectra (Figure 4-5) at binding energies of 586 and 576.0 eV, which correspond to the Cr $2p_{1/2}$ and Cr $2p_{3/2}$ signals, respectively [76]. The O 1s spectra of HEO-Air and HEO-Ar are shown in Figure 4-7. The usual lattice oxygen is represented by the OL peak at 529.5 eV, while the oxygen vacancy (Ov) peak is represented by the OL peak at 531.2 eV [60, 64]. The quantity of oxygen vacancies in the structure is shown to rise as the oxygen content of the synthesis environment lowers. The samples that were calcined in Ar exhibit somewhat more oxygen vacancies than those that were calcined in the Air environment.

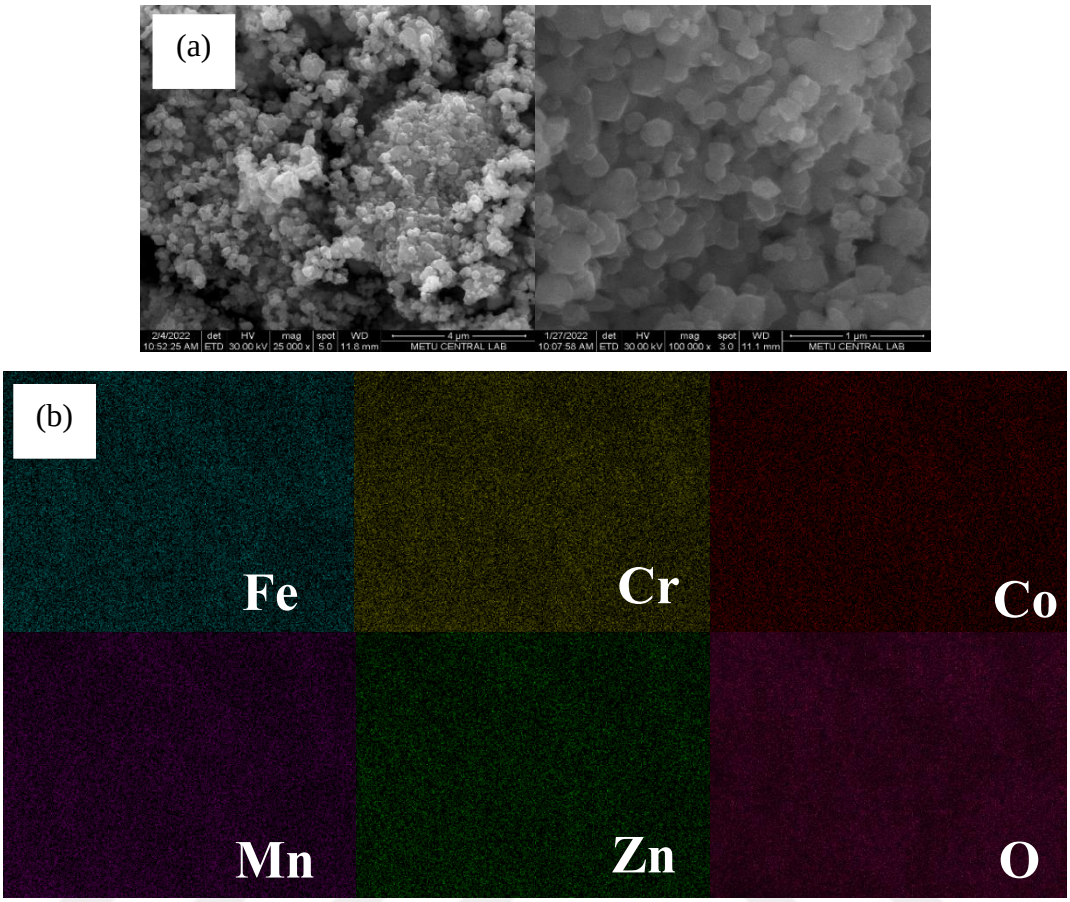

Figure 4-4: SEM image (a) and EDX mapping (b) of elements constituting HEO-Ar, EDX mapping conducted using 25 000x magnified image [77]

Figure 4-8 displays the initial discharge-charge curves for the HEO-Ar and HEO-Air electrodes at a current density of 100 mA/g. Initial discharge capabilities for the HEO-Ar and HEO-Air electrodes are 1234 and 1270 mAh/g, respectively. The two areas of the electrodes' discharge activity are comparable.

The creation of the solid electrolyte interphase (SEI) at the electrolyte and electrode interface is shown by the first area (0.86-0.54 V), which also shows the incorporation of Li^+ ions into the structure [60, 65, 66] Transition metal oxides in the HEO interact with Li^+ through a conversion process in the second area below 0.54 V, resulting in the formation of Li_2O and metallic states for the transition metal oxides [60, 65]. Figure 4-8 shows that the electrodes' initial charge behavior is likewise comparable.

The HEO-Ar and HEO-Air electrodes have initial coulombic efficiencies of 71.8% and 72.4%, respectively.

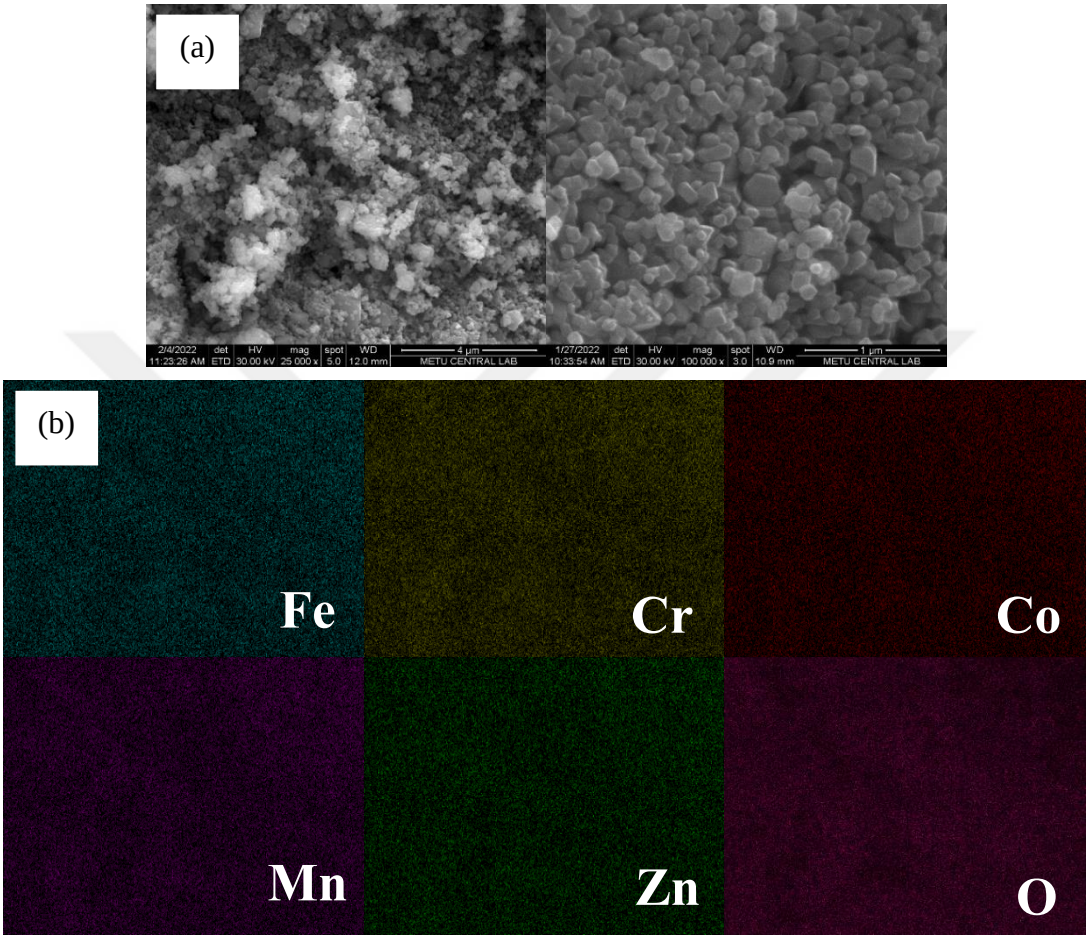

Figure 4-5: SEM image (a) and EDX mapping (b) of elements constituting HEO-Air, EDX mapping conducted using 25 000x magnified image [77]

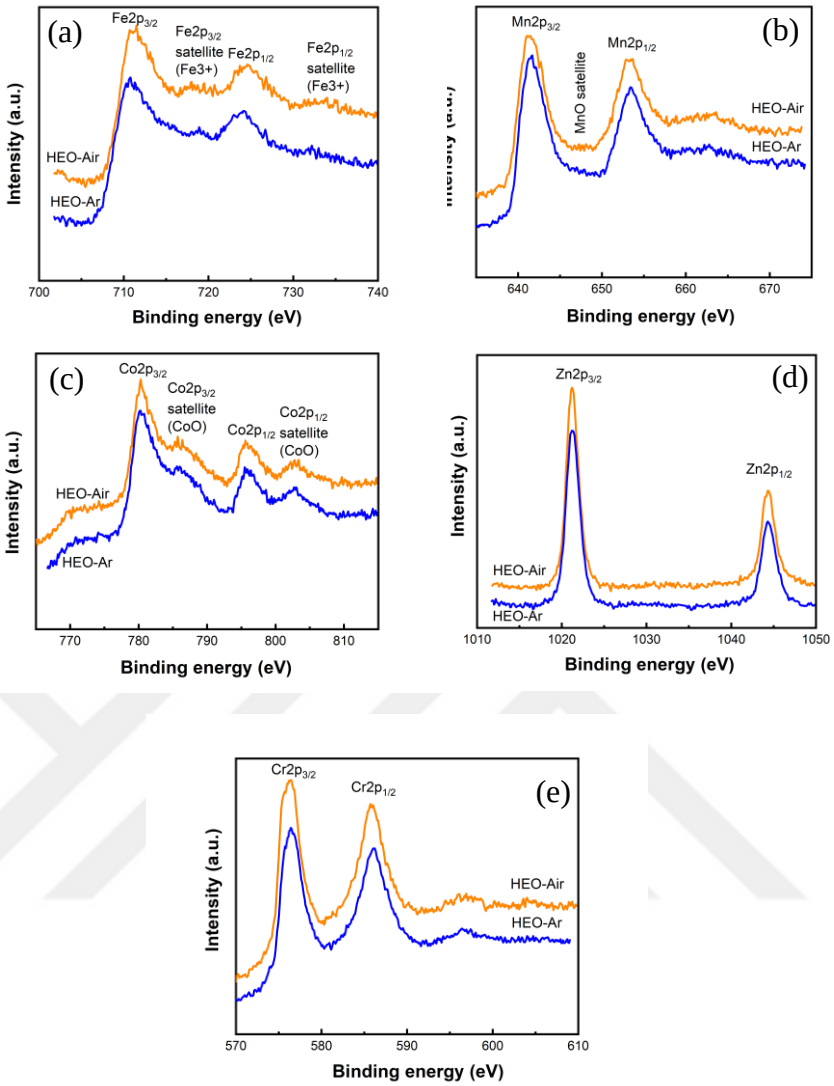

Figure 4-6: XPS core level spectra of (a) Fe 2p , (b) Mn 2p, (c) Co 2p, (d) Zn 2p and (e) Cr 2p [77]

The HEO-Ar and HEO-Air electrodes' CV curves are shown in Figure 4-9 for the first two cycles at a rapid scan rate of 2 mV s^{-1}. The early lithiation process, which involves the development of the SEI layer and structural changes, can be linked to a discernible reduction peak with a rather high current density during the first cathodic scan. The reduction processes of the (A) HEO-Ar and (B) HEO-Air powders' XPS O 1s spectra are shown in Figure 4-7. The structural change in the electrode consists of 5 electrochemically active metal cations. The peak at 1.54 V in the first anodic scan is connected to the oxidation processes of the respective metals [46, 67]. The

reduction and oxidation peaks in the following cycle are situated at 0.6 and 1.67 V, respectively. While this is happening, Zn and Li alloy under 0.25 V during the reduction process (lithiation) [68]. However, the rapid scan rate CV tests do not reveal the reversible dealloying oxidation peak.

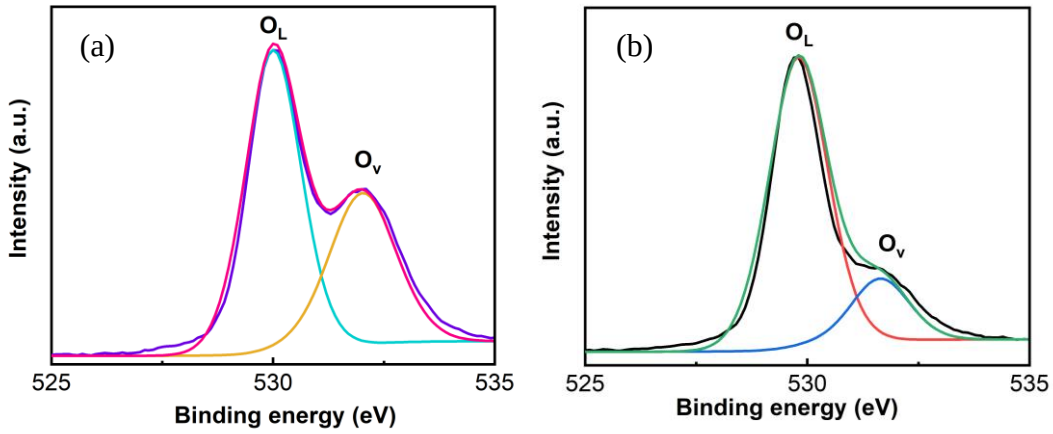

Figure 4-7: XPS core level spectra of O 1s for (a) HEO-Ar, and (b) HEO-Air [77]

The electrodes' cycle and rate performances at 100, 500, and 1000 mA g^{-1} current densities Figure 4-10 shows the plotting of 80 cycles. The discharge capabilities of the HEO-Ar and HEO-Air electrodes were 714 and 544 mAh/g, respectively, at the conclusion of the first 20th cycle at 100 mA/g. Figure 4-9 makes this point quite evident. During this time, the HEO-Air electrode rapidly loses capacity. Electrodes behave more consistently as the current rate rises, although the capacity of the HEO-Ar electrode is still 1.25 times more than that of the HEO-Air electrode. The discharge capabilities of the HEO-Ar and HEO-Air electrodes are 351 and 275 mAh/g, respectively, at the current density of 1000 mA/g. The HEO-Ar electrode has a reversible discharge capacity of 548 mAh/g, which is larger than that of the HEO-Air electrode (411 mAh/g) when the current density ultimately drops to 100 mA/g.

Figure 4-11 shows the electrodes' electrochemical impedance spectra at the open circuit voltage before the cycle testing. The electrochemical impedance spectrum of the electrode is fitted using the equivalent circuit model that is depicted as an inset

in Figure 4-11 (b). The solution resistance, SEI film resistance, charge transfer resistance, constant phase element linked to capacitance operations, and Warburg impedance resulting from Li^+ migration are all represented in this model by the letters R_s, R_{film}, R_{ct}, CPE, and W, respectively. The R_{ct} values for the HEO-Ar and HEO-Air electrodes, respectively, are determined to be 133.5 and 168.2 at the electrode/electrolyte interface. Figure 4-11 (b) displays the electrodes' Nyquist plots following the 80th cycle. Both electrodes' R_{ct} values have been drastically decreased. This phenomenon is linked to the material's electrochemical activation [60, 69]. Reduced metallic conversion products rise in the anode during charge-discharge cycling. As a result, electrodes' surface conductivity rises. Charge transfer resistance lowers as the anode's conductivity rises. It is clear from the low Rct value and the Warburg line slope that the HEO-Ar electrode displays quicker Li^+ diffusion than the other electrodes when compared to HEO-Air electrode tested in this work [70].

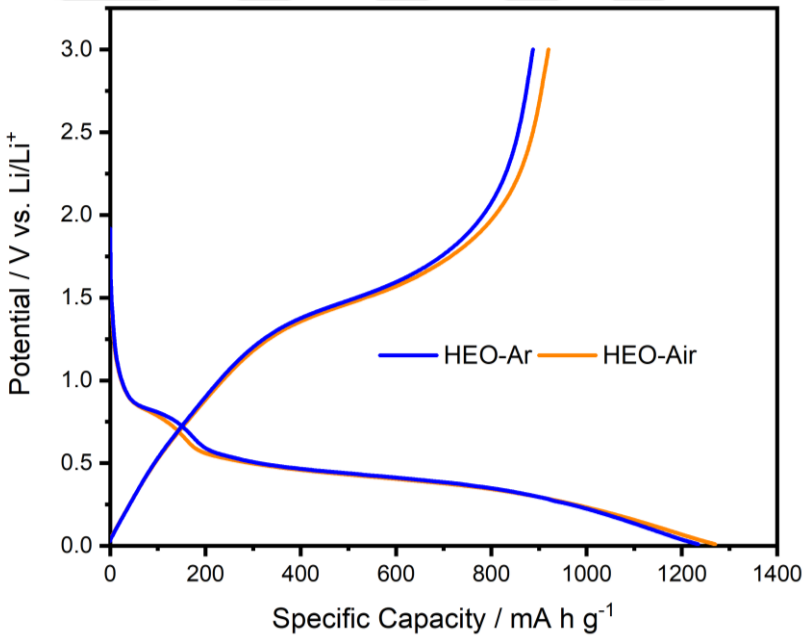

Figure 4-8: First charge and discharge voltage profiles of HEO-Ar and HEO-Air at a current rate of 100 mA/g [77]

The results of GITT measurements were used to better understand the electrochemical kinetics and identify the lithium diffusion coefficient (DLi^+) of the

electrodes. The resulting curves are presented in Figures 4-12 (a) and 4-12 (b). It is discovered to be 2.52x10^{-11} cm^2/s for the HEO-Ar electrode and 7.09x10^{-13} cm^2/s for the HEO-Air electrode, respectively. The HEO-Ar sample exhibits a DLi$^+$ value that is 30 times greater than that of the HEO-Air sample, which may be attributed to the accelerated diffusion kinetics brought on by the many oxygen vacancies.

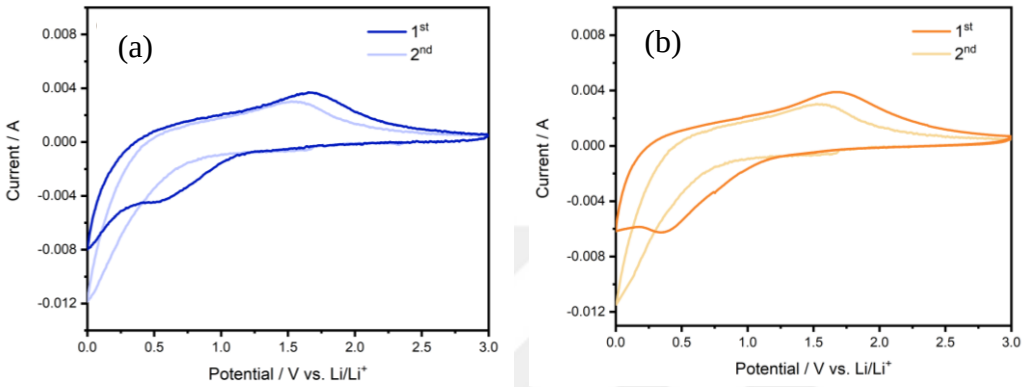

Figure 4-9: Cyclic voltammetry measurements at a scan rate of 2.0 mV/s of (a) HEO-Ar, and (b) HEO-Air [77]

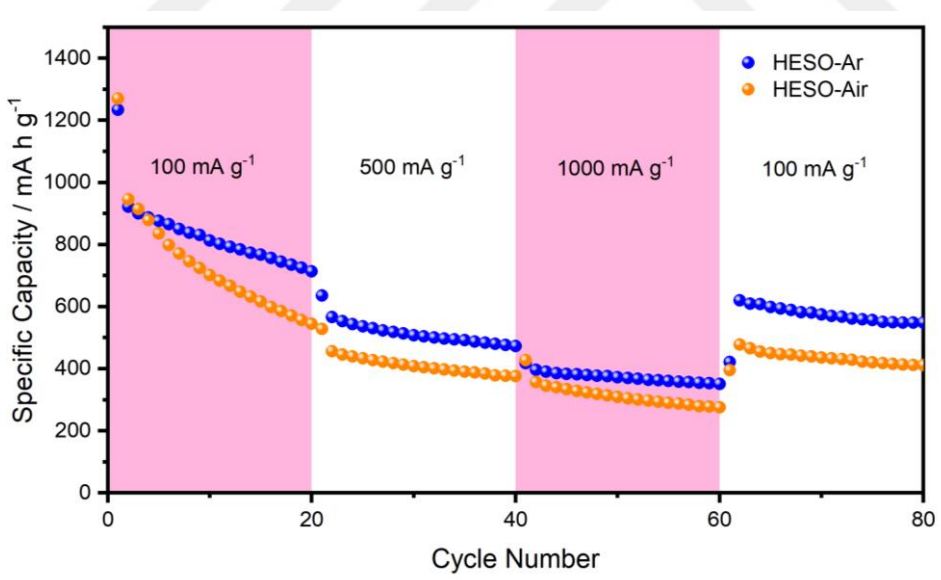

Figure 4-10: Cycle test of the HEO materials under different current rates [77]

The greater interplanar spacing may be utilized to explain the acceleration of Li$^+$ diffusion brought on by the presence of oxygen vacancies (Figure 4-1 and Table 4-1). The diffusion coefficients of comparable high entropy oxide-based electrodes

have been seen to vary in the literature in the range of 10^{-11} to 10^{-15} cm^2/s [46, 67, 71]. The electrode material's high lithium diffusion coefficient suggests that the reaction requirement may be satisfied, and improved performance can be attained at high currents.

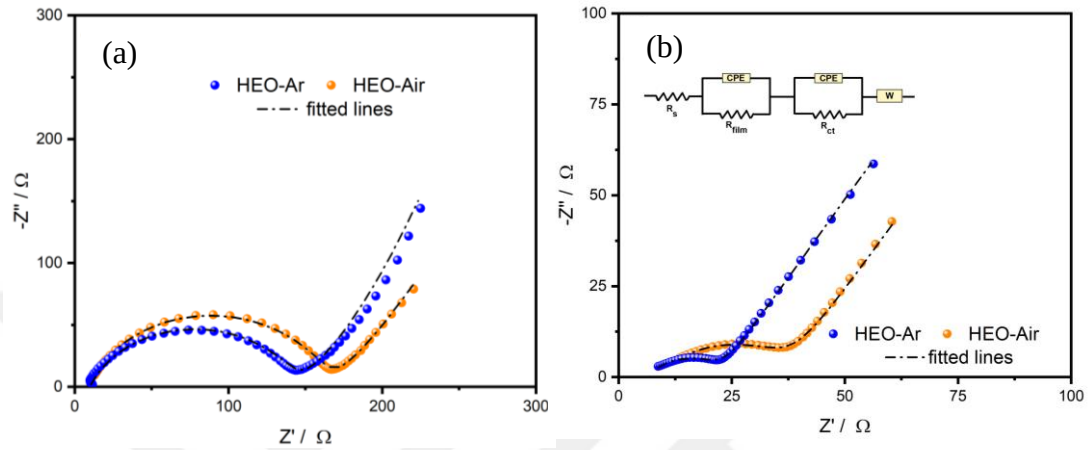

Figure 4-11: Nyquist plots of EIS measurements of HEO-Ar and HEO-Air before (a) and after (b) 80 cycles [77]

For the HEO-Ar sample, additional CV tests at various scan rates were carried out in order to compare the DLi^+ from the GITT analysis. Figure 4-13 shows that the current intensity of the peaks rises as the scan rate rises, and no peak position shifts are significant, confirming excellent rate performance [72, 73]. In general, the b value in the equation, which reflects the connection between current and scan rate (indicated in Figure 4-13), may be used to obtain kinetic information. Diffusion-controlled and capacitive processes, respectively, are indicated by b values of 0.5 and 1, respectively. The b values for peak 1 (P1) and peak 2 (P2) were computed as 0.96 and 0.94, respectively, as shown in Figure 4-13 (b). Li^+ insertion/extraction operations dominate the capacitive process. In other words, the electrode/electrolyte contact is readily reactive with Li^+ [72, 73]. Additionally, it is crucial for LIBs' HEO-based electrodes to work at greater rates.

The generated CV curves are also assessed in order to look into the kinetics of lithium diffusion in the HEO-Ar electrode. According to the scan rate, the peak currents in the CV for oxidation and reduction processes fluctuate.

Understanding the diffusion kinetics of lithium at the electrode/electrolyte contact is made possible by this. According to the Randles-Sevcik equation [74], relationship and chemical lithium diffusion coefficient (DLi $^{+}$) may be calculated.

$$i_p = (2.69x10^5)n^{\frac{3}{2}}AD_{Li^+}^{\frac{1}{2}}C_{Li^+}^{*}\vartheta^{\frac{1}{2}} \quad \text{(Equation 7)}$$

i_p stands for peak current, n for HEO-Ar charge transfer number, A for electrode and electrolyte contact area, $C_{Li^+}^{*}$for bulk concentration of lithium in the electrode, and ϑ for scan rate. The equation shows a linear relationship between the peak current and the square root of the scan rate. Tables 4-2, 4-3 and 4-4 lists the D_{Li^+} values estimated for the HEO-Ar and HEO-Air electrode at various scan speeds together with the D_{Li^+} value determined using GITT measurements. Overall, it is evident that the D_{Li^+} derived independently from the CV and GITT analyses are complementary.

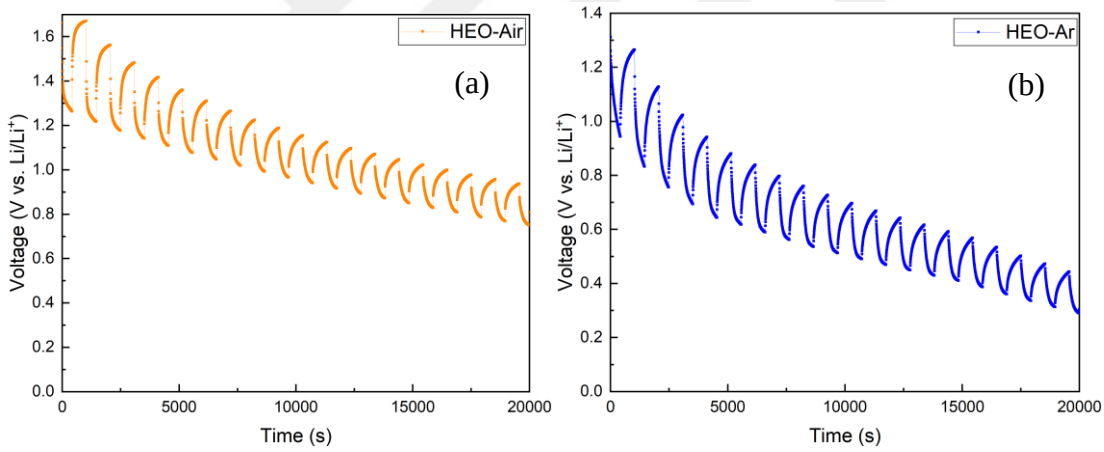

Figure 4-12: GITT measurements of HEO-Air (a) and HEO-Ar (b) [77]

D_{Li^+} using GITT was computed via the Equation 8. In this equation τ denotes current pulse time, m, V, M are referring to the mass, the molar volume, and the molar mass of the material respectively. S is the electrode – electrolyte interface area. For the simplicity of computation, it is assumed as the electrode area. ΔE_S is the change of the steady state voltage during a single pulse. ΔE_t is the difference in the cell voltage after a pulse current, neglecting the IR drop [78].

$$D_{Li^+} = \frac{4}{\pi\tau}\left(\frac{mV}{MS}\right)^2\left(\frac{\Delta E_S}{\Delta E_t}\right)^2 \quad \text{(Equation 8)}$$

Table 4-2: Computed DLi^+ values using 0.25 mV/s and 0.50 mV/s scan-rate for HEO-Ar

Method	**CV (0.25 mV/s -P1)**	**CV (0.25 mV/s -P2)**	**CV (0.50 mV/s -P1)**	**CV (0.50 mV/s -P2)**
Material	HEO-Ar	HEO-Ar	HEO-Ar	HEO-Ar
DLi^+ (cm^2/s)	9.02×10^{-11}	2.94×10^{-11}	6.18×10^{-11}	3.76×10^{-11}

Table 4-3: Computed DLi+ values using 0.75 mV/s and 1.00 mV/s scan-rate for HEO-Ar

Method	**CV (0.75 mV/s -P1)**	**CV (0.75 mV/s -P2)**	**CV (1.00 mV/s -P1)**	**CV (1.00 mV/s -P2)**
Material	HEO-Ar	HEO-Ar	HEO-Ar	HEO-Ar
DLi^+ (cm^2/s)	8.23×10^{-11}	5.17×10^{-11}	1.21×10^{-11}	1.02×10^{-11}

Table 4-4: Computed DLi^+ values using GITT measurements for HEO-Ar and HEO-Air

Method	**GITT**	**GITT**
Material	HEO-Ar	HEO-Air
DLi^+ (cm^2/s)	2.52×10^{-11}	7.09×10^{-13}

According to Randles-Sevcik equation the peak current has a linear relationship with the square root of voltage scan rate. It can be assumed that i_p and v have a power-law relationship [79, 80]. Using this assumption equation can be rearranged to the following equations.

$$i_p = av^b \quad \text{(Equation 9)}$$

$$\log(i_p) = b\log(v) + \log a \qquad \text{(Equation 10)}$$

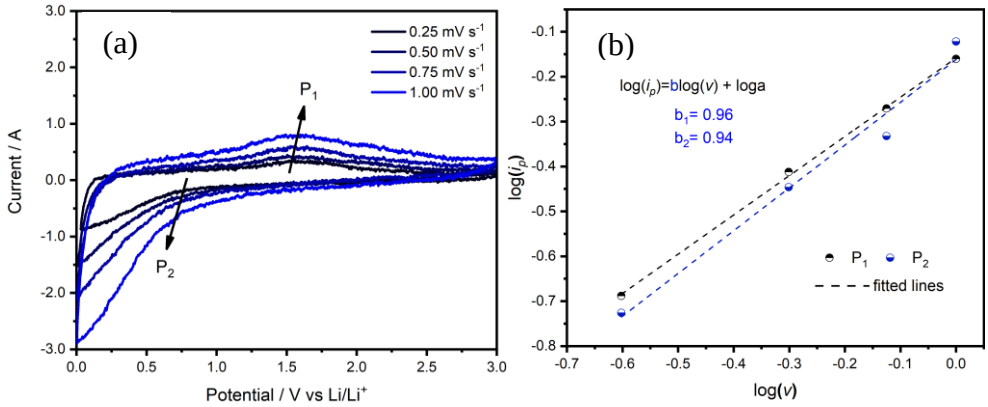

Figure 4-13: CV curves of HEO-Ar at different scan rates overlapped (a), log(v) vs log(ip) plot (b) [77]

For these equations a and b are variables. The b value provides information regarding the charge storage mechanism. When equation 10 is plotted just like in Figure 4-13 (b), b value is obtained from the derivative of the line. For this condition b is expected to have a figure between 0.5 and 1.0. The former figure suggests that the charge storage mechanism process is a faradaic intercalation and is dominated by a semi-infinite linear diffusion. The latter figure of 1.0 is indicative of a surface capacitive charge storage mechanism for which the effect of diffusion may be negligible [72]. As shown in the results of this study, b figures are 0.96 and 0.94 for P1 and P2 peaks respectively. These results indicate that lithium storage on the active material of $(FeMnCrCoZn)_3O_4$ is controlled by surface redox processes. Hence the lithium diffusion coefficient calculations are complemented by using GITT.

Another method with which lithium diffusion coefficient calculations can be done is Potentiostatic intermittent titration technique (PITT). PITT has the advantage of avoidance of nucleation of new phases given the electrode potential is controlled in the range of single phase potential window [81]. Lithium diffusion coefficient is computed via PITT using the following formula:

$$D_{Li^+} = \left(\frac{(I\sqrt{t})_{max}\sqrt{\pi}r_1}{\Delta Q}\right)^2 \qquad \text{(Equation 11)}$$

where t is the process time, r_1 is active material radius, ΔQ is the total charge transferred during the process; derived using Cottrell boundary conditions of infinitely fast kinetics, linear diffusion, and semi-infinite thickness [82]. Deiss (2002) claims that D_{Li^+} calculation around the CV peak potentials exhibits an erroneous potential dependance, calls for improved analysis and boundary condition selection [82]. In the later report of Deiss (2004) a similar phenomenon is observed for GITT method as well [78].

During this work for the purpose of complimenting electrochemical performance results GITT method was used to compute D_{Li^+}. Computation was conducted by the data obtained from the 2nd lithiation cycle, so that the effect of SEI formation can be neglected, assuming SEI layer formation is completed in the first cycle. One of the problems that could be encountered is that due to unrefined fabrication process of HEO material its particle size distribution is believed to have a large distribution, although not being quantitative SEM images supports this claim. Therefore, employing PITT in this scenario could have led to inconsistencies in the results. For future works it can be advised that both GITT and PITT may be used to compute lithium diffusion data, in addition to computation via CV and EIS. However, computation of D_{Li^+} along the whole voltage window both lithiation and delithiation will allow for healthier comparison with literature.

CHAPTER 5

CONCLUSIONS AND FUTURE WORK

In this study, the impact of the synthesis environment argon and air on the structural and electrochemical characteristics of powders of $(FeMnCrCoZn)_3O_4$ (HEO) is examined. It has been demonstrated that HEO-Ar produced using a high entropy approach has improved electrochemical performance. Better electrochemical performances are achieved as a result of the oxygen vacancies in the HEO-Ar sample, which has increased number of sites for Li+ accommodation, decreased impedance, and accelerated Li^+ diffusion kinetics compared to HEO-Air. These materials are still far away from commercialization. However, it has the potential to be tailor-made specific to the use and consumer needs. Compared to the current active materials utilized for electrochemical energy storage, HEOs provide several potentially favorable characteristics. The materials' inherent characteristics make their attributes variable. By altering the composition and stoichiometry of the components, these materials can be precisely created to satisfy the requirements of the application.

- By changing the oxygen vacancy properties higher performance active materials are produced compared to the ones synthesized in air. Lithium diffusivity coefficient of 2.52×10^{-11} cm^2/s and 7.09×10^{-13} cm^2/s have been observed for HEO-Ar and HEO-Air respectively.
- Equimolar high entropy oxides show significantly better properties in terms of capacity to conventional graphite's theoretical 372 mAh/g specific capacity. Specific capacities of 548 mAh/g and 351 mAh/g have been achieved under 100 mA/g and 1000 mA/g current rates using HEO-Ar.
- Compared to conventional graphite and silicon-based materials HEOs show higher voltage, which decreases the energy density. However, if HEOs are

used against a conventional cathode material like NMC, LFP the full cell can be discharged up to 0 Volts which is a passive safety feature for full cells.

- Thanks to their high current rate capabilities and long cycle life these materials have the potential to be used in grid level applications, such as peak shaving, grid support and renewable energy storage.

Both in this work and the literature, HEOs exhibit improved capacity, rate capability, and capacity retention qualities. Better performance in real-world applications may then be made possible by these improvements and continued research. Further studies are necessary for better understanding of lithium storage mechanism . Post-mortem analysis of the electrodes may enable the understanding of structural and compositional changes in the active material. Which will enable for a better material design.

REFERENCES

1- Goodenough, J. B., & Kim, Y. (2009). Challenges for rechargeable Li Batteries. Chemistry of Materials, 22(3), 587–603. https://doi.org/10.1021/cm901452z

2- Enerji Depolama Sistemi - ASPİLSAN. ASPİLSAN - Teknolojinin Enerjisi. (2023, June 13). https://www.aspilsan.com/en/cozumler/enerji-depoloma/enerji-depolama-sistemi/

3- Lithium-Ion Batteries. Panasonic. (n.d.). https://industrial.panasonic.com/ww/products/pt/lithium-ion

4- Weber, A. Z., Mench, M. M., Meyers, J. P., Ross, P. N., Gostick, J. T., & Liu, Q. (2011). Redox Flow Batteries: A Review. Journal of Applied Electrochemistry, 41(10), 1137–1164. https://doi.org/10.1007/s10800-011-0348-2

5- Pandolfo, A. G., & Hollenkamp, A. F. (2006). Carbon properties and their role in Supercapacitors. Journal of Power Sources, 157(1), 11–27. https://doi.org/10.1016/j.jpowsour.2006.02.065

6- Jia, C., Pan, F., Zhu, Y. G., Huang, Q., Lu, L., & Wang, Q. (2015). High–energy density nonaqueous all redox flow lithium battery enabled with a polymeric membrane. Science Advances, 1(10). https://doi.org/10.1126/sciadv.1500886

7- Kumar, A., & Sehgal, M. (2018). Hydrogen fuel cell technology for a sustainable future: A Review. SAE Technical Paper Series. https://doi.org/10.4271/2018-01-1307

8- Toyota Fuel Cell Electric vehicles: Toyota Europe. Toyota EU. (n.d.). https://www.toyota-europe.com/electrification/fcev

9- Götz, M., Lefebvre, J., Mörs, F., McDaniel Koch, A., Graf, F., Bajohr, S., Reimert, R., & Kolb, T. (2016). Renewable power-to-gas: A technological and Economic

Review. Renewable Energy, 85, 1371–1390. https://doi.org/10.1016/j.renene.2015.07.066

10- Zakeri, B., & Syri, S. (2015). Electrical Energy Storage Systems: A comparative life cycle cost analysis. Renewable and Sustainable Energy Reviews, 42, 569–596. https://doi.org/10.1016/j.rser.2014.10.011

11- Pumped storage and large pumping plants. Black & Veatch. (n.d.). https://www.bv.com/industries/hydropower-hydraulic-structures/pumped-storage-hydropower

12- Nzereogu, P. U., Omah, A. D., Ezema, F. I., Iwuoha, E. I., & Nwanya, A. C. (2022). Anode materials for lithium-ion batteries: A Review. Applied Surface Science Advances, 9, 100233. https://doi.org/10.1016/j.apsadv.2022.100233

13- Obrovac, M. N., & Christensen, L. (2004). Structural changes in silicon anodes during lithium insertion/extraction. Electrochemical and Solid-State Letters, 7(5). https://doi.org/10.1149/1.1652421

14- Weijie Wang, Zuqin Liu, Song Han, Jonathan Bornstein, Constantin Ionel Stefan, (2015), Structurally controlled deposition of silicon onto nanowires, (WO2015175509A1), https://patents.google.com/patent/WO2015175509A1/en

15- BTR New Material Group Co., ltd.. (n.d.). https://www.btrchina.com/en/NegativeProducts/info.aspx?itemid=1068

16- Cheng, X.-B., Zhang, R., Zhao, C.-Z., & Zhang, Q. (2017). Toward safe lithium metal anode in rechargeable batteries: A Review. Chemical Reviews, 117(15), 10403–10473. https://doi.org/10.1021/acs.chemrev.7b00115

17- Markevich, E., Salitra, G., Hartmann, P., Kulisch, J., Aurbach, D., Park, K.-J., Yoon, C. S., & Sun, Y.-K. (2019). New insights related to rechargeable lithium batteries: Li metal anodes, ni rich LinixcoymnzO2 cathodes and beyond them. Journal of The Electrochemical Society, 166(3). https://doi.org/10.1149/2.0261903jes

18- Mizushima, K., Jones, P. C., Wiseman, P. J., & Goodenough, J. B. (1980). LixCoO2 (0<x<-1): A new cathode material for batteries of high energy density. Materials Research Bulletin, 15(6), 783–789. https://doi.org/10.1016/0025-5408(80)90012-4

19- Padhi, A. K., Nanjundaswamy, K. S., & Goodenough, J. B. (1997). Phospho-Olivines as positive-electrode materials for rechargeable lithium batteries. Journal of The Electrochemical Society, 144(4), 1188–1194. https://doi.org/10.1149/1.1837571

20- Lu, L., Han, X., Li, J., Hua, J., & Ouyang, M. (2013). A review on the key issues for lithium-ion battery management in Electric Vehicles. Journal of Power Sources, 226, 272–288. https://doi.org/10.1016/j.jpowsour.2012.10.060

21- Purwanto, A., Yudha, C. S., Ubaidillah, U., Widiyandari, H., Ogi, T., & Haerudin, H. (2018). NCA cathode material: Synthesis methods and performance enhancement efforts. Materials Research Express, 5(12), 122001. https://doi.org/10.1088/2053-1591/aae167

22- Xu, J., Dou, S., Liu, H., & Dai, L. (2013). Cathode materials for next generation lithium ion batteries. Nano Energy, 2(4), 439–442. https://doi.org/10.1016/j.nanoen.2013.05.013

23- Zhang, S. S. (2007). A review on the separators of liquid electrolyte li-ion batteries. Journal of Power Sources, 164(1), 351–364. https://doi.org/10.1016/j.jpowsour.2006.10.065

24- Celgard® 2400 monolayer microporous membrane. (n.d.). https://www.celgard.com/storage/components/2400_com_october2021_20033.pdf

25- Gogia, A., Wang, Y., Rai, A. K., Bhattacharya, R., Subramanyam, G., & Kumar, J. (2021). Binder-free, thin-film ceramic-coated separators for improved safety of lithium-ion batteries. ACS Omega, 6(6), 4204–4211. https://doi.org/10.1021/acsomega.0c05037

26- Mun, J., Yim, T., Gap Kwon, Y., & Jae Kim, K. (2021). Self-assembled nano-silica-embedded polyethylene separator with outstanding physicochemical and thermal properties for advanced sodium ion batteries. Chemical Engineering Journal, 405, 125844. https://doi.org/10.1016/j.cej.2020.125844

27- Wang, C., Adair, K., & Sun, X. (2021). All-solid-state lithium metal batteries with sulfide electrolytes: Understanding interfacial ion and Electron Transport. Accounts of Materials Research, 3(1), 21–32. https://doi.org/10.1021/accountsmr.1c00137

28- Separator product portfolio - ENTEK. (n.d.-b). https://entek.com/wp-content/uploads/2021/05/Lithium-Prod-Portfolio-21-04-23.pdf

29- Xu, K. (2004). Nonaqueous liquid electrolytes for lithium-based rechargeable batteries. Chemical Reviews, 104(10), 4303–4418. https://doi.org/10.1021/cr030203g

30- Winter, M., & Brodd, R. J. (2004). What are batteries, fuel cells, and supercapacitors? Chemical Reviews, 104(10), 4245–4270. https://doi.org/10.1021/cr020730k

31- Matsumoto, K., Inoue, K., Nakahara, K., Yuge, R., Noguchi, T., & Utsugi, K. (2013). Suppression of aluminum corrosion by using high concentration litfsi electrolyte. Journal of Power Sources, 231, 234–238. https://doi.org/10.1016/j.jpowsour.2012.12.028

32- Lewandowski, A., & Świderska-Mocek, A. (2009). Ionic liquids as electrolytes for Li-ion batteries—an overview of electrochemical studies. Journal of Power Sources, 194(2), 601–609. https://doi.org/10.1016/j.jpowsour.2009.06.089

33- Lu, C., & Chen, X. (2022). Learn from nature: Bio-inspired structure design for lithium-Ion Batteries. EcoMat, 4(3). https://doi.org/10.1002/eom2.12181

34- Juarez-Robles, D., Vyas, A. A., Fear, C., Jeevarajan, J. A., & Mukherjee, P. P. (2020). Overcharge and aging analytics of Li-ion cells. Journal of The

Electrochemical Society, 167(9), 090547. https://doi.org/10.1149/1945-7111/ab9569

35- Yeh, J.-W., Chen, S.-K., Lin, S.-J., Gan, J.-Y., Chin, T.-S., Shun, T.-T., Tsau, C.-H., & Chang, S.-Y. (2004). Nanostructured High-entropy alloys with multiple principal elements: Novel Alloy Design Concepts and outcomes. Advanced Engineering Materials, 6(5), 299–303. https://doi.org/10.1002/adem.200300567

36- Cantor, B., Chang, I. T. H., Knight, P., & Vincent, A. J. B. (2004). Microstructural development in equiatomic multicomponent alloys. Materials Science and Engineering: A, 375–377, 213–218. https://doi.org/10.1016/j.msea.2003.10.257

37- George, E. P., Raabe, D., & Ritchie, R. O. (2019). High-entropy alloys. Nature Reviews Materials, 4(8), 515–534. https://doi.org/10.1038/s41578-019-0121-4

38- Moskovskikh, D., Vorotilo, S., Buinevich, V., Sedegov, A., Kuskov, K., Khort, A., Shuck, C., Zhukovskyi, M., & Mukasyan, A. (2020). Extremely hard and tough high entropy nitride ceramics. Scientific Reports, 10(1). https://doi.org/10.1038/s41598-020-76945-y

39- Sarker, P., Harrington, T., Toher, C., Oses, C., Samiee, M., Maria, J.-P., Brenner, D. W., Vecchio, K. S., & Curtarolo, S. (2018). High-entropy high-hardness metal carbides discovered by entropy descriptors. Nature Communications, 9(1). https://doi.org/10.1038/s41467-018-07160-7

40- Sarkar, A., Breitung, B., & Hahn, H. (2020). High entropy oxides: The role of entropy, enthalpy and Synergy. Scripta Materialia, 187, 43–48. https://doi.org/10.1016/j.scriptamat.2020.05.019

41- Sarkar, A., Velasco, L., Wang, D., Wang, Q., Talasila, G., de Biasi, L., Kübel, C., Brezesinski, T., Bhattacharya, S. S., Hahn, H., & Breitung, B. (2018). High entropy oxides for reversible energy storage. Nature Communications, 9(1). https://doi.org/10.1038/s41467-018-05774-5

42- Wang, T., Chen, H., Yang, Z., Liang, J., & Dai, S. (2020). High-entropy perovskite fluorides: A new platform for oxygen evolution catalysis. Journal of the American Chemical Society, 142(10), 4550–4554. https://doi.org/10.1021/jacs.9b12377

43- Mao, A., Xiang, H.-Z., Zhang, Z.-G., Kuramoto, K., Yu, H., & Ran, S. (2019). Solution combustion synthesis and magnetic property of rock-salt (co0.2cu0.2mg0.2ni0.2zn0.2)o high-entropy oxide nanocrystalline powder. Journal of Magnetism and Magnetic Materials, 484, 245–252. https://doi.org/10.1016/j.jmmm.2019.04.023

44- Wang, J., Stenzel, D., Azmi, R., Najib, S., Wang, K., Jeong, J., Sarkar, A., Wang, Q., Sukkurji, P. A., Bergfeldt, T., Botros, M., Maibach, J., Hahn, H., Brezesinski, T., & Breitung, B. (2020). Spinel to rock-salt transformation in high entropy oxides with Li Incorporation. Electrochem, 1(1), 60–74. https://doi.org/10.3390/electrochem1010007

45- Lin, L., Wang, K., Azmi, R., Wang, J., Sarkar, A., Botros, M., Najib, S., Cui, Y., Stenzel, D., Anitha Sukkurji, P., Wang, Q., Hahn, H., Schweidler, S., & Breitung, B. (2020). Mechanochemical Synthesis: Route to novel rock-salt-structured high-entropy oxides and oxyfluorides. Journal of Materials Science, 55(36), 16879–16889. https://doi.org/10.1007/s10853-020-05183-4

46- Nguyen, T. X., Patra, J., Chang, J.-K., & Ting, J.-M. (2020). High entropy spinel oxide nanoparticles for superior lithiation–delithiation performance. Journal of Materials Chemistry A, 8(36), 18963–18973. https://doi.org/10.1039/d0ta04844e

47- Commodity markets. World Bank. (n.d.). https://www.worldbank.org/en/research/commodity-markets

48- Wang, Q., Sarkar, A., Li, Z., Lu, Y., Velasco, L., Bhattacharya, S. S., Brezesinski, T., Hahn, H., & Breitung, B. (2019). High entropy oxides as anode material for Li-ion battery applications: A practical approach. Electrochemistry Communications, 100, 121–125. https://doi.org/10.1016/j.elecom.2019.02.001

49- George, E. P., Raabe, D., & Ritchie, R. O. (2019). High-entropy alloys. Nature Reviews Materials, 4(8), 515–534. https://doi.org/10.1038/s41578-019-0121-4

50- Zhang, M., George, E. P., & Gibeling, J. C. (2021). Tensile creep properties of a CrMnFeCoNi high-entropy alloy. Scripta Materialia, 194, 113633. https://doi.org/10.1016/j.scriptamat.2020.113633

51- Ye, Y. F., Wang, Q., Lu, J., Liu, C. T., & Yang, Y. (2016). High-entropy alloy: Challenges and prospects. Materials Today, 19(6), 349–362. https://doi.org/10.1016/j.mattod.2015.11.026

52- Ma, Y., Ma, Y., Wang, Q., Schweidler, S., Botros, M., Fu, T., Hahn, H., Brezesinski, T., & Breitung, B. (2021). High-entropy energy materials: Challenges and new opportunities. Energy & Environmental Science, 14(5), 2883–2905. https://doi.org/10.1039/d1ee00505g

53- Albedwawi, S. H., AlJaberi, A., Haidemenopoulos, G. N., & Polychronopoulou, K. (2021). High entropy oxides-exploring a paradigm of promising catalysts: A Review. Materials & Design, 202, 109534. https://doi.org/10.1016/j.matdes.2021.109534

54- Rost, C. M., Sachet, E., Borman, T., Moballegh, A., Dickey, E. C., Hou, D., Jones, J. L., Curtarolo, S., & Maria, J.-P. (2015). Entropy-stabilized oxides. Nature Communications, 6(1). https://doi.org/10.1038/ncomms9485

55- Ma, Y., Ma, Y., Wang, Q., Schweidler, S., Botros, M., Fu, T., Hahn, H., Brezesinski, T., & Breitung, B. (2021a). High-entropy energy materials: Challenges and new opportunities. Energy & Environmental Science, 14(5), 2883–2905. https://doi.org/10.1039/d1ee00505g

56- Yu, S.-H., Feng, X., Zhang, N., Seok, J., & Abruña, H. D. (2018). Understanding conversion-type electrodes for lithium rechargeable batteries. Accounts of Chemical Research, 51(2), 273–281. https://doi.org/10.1021/acs.accounts.7b00487

57- Sarkar, A., Wang, Q., Schiele, A., Chellali, M. R., Bhattacharya, S. S., Wang, D., Brezesinski, T., Hahn, H., Velasco, L., & Breitung, B. (2019). High-entropy oxides: Fundamental aspects and electrochemical properties. Advanced Materials, 31(26), 1806236. https://doi.org/10.1002/adma.201806236

58- Wang, J., Cui, Y., Wang, Q., Wang, K., Huang, X., Stenzel, D., Sarkar, A., Azmi, R., Bergfeldt, T., Bhattacharya, S. S., Kruk, R., Hahn, H., Schweidler, S., Brezesinski, T., & Breitung, B. (2020). Lithium containing layered high entropy oxide structures. Scientific Reports, 10(1). https://doi.org/10.1038/s41598-020-75134-1

59- Duan, C., Tian, K., Li, X., Wang, D., Sun, H., Zheng, R., Wang, Z., & Liu, Y. (2021). New spinel high-entropy oxides (feconicrmnxli)3o4 (x = Cu, Mg, Zn) as the anode material for lithium-ion batteries. Ceramics International, 47(22), 32025–32032. https://doi.org/10.1016/j.ceramint.2021.08.091

60- Lökçü, E., Toparli, Ç., & Anik, M. (2020). Electrochemical performance of (mgconizn)1–xlixO high-entropy oxides in lithium-ion batteries. ACS Applied Materials & Interfaces, 12(21), 23860–23866. https://doi.org/10.1021/acsami.0c03562

61- Osenciat, N., Bérardan, D., Dragoe, D., Léridon, B., Holé, S., Meena, A. K., Franger, S., & Dragoe, N. (2019). Charge compensation mechanisms in Li-substituted high-entropy oxides and influence on Li superionic conductivity. Journal of the American Ceramic Society, 102(10), 6156–6162. https://doi.org/10.1111/jace.16511

62- Biesinger, M. C., Payne, B. P., Grosvenor, A. P., Lau, L. W. M., Gerson, A. R., & Smart, R. St. C. (2011). Resolving surface chemical states in XPS analysis of first row transition metals, oxides and hydroxides: CR, Mn, Fe, Co and Ni. Applied Surface Science, 257(7), 2717–2730. https://doi.org/10.1016/j.apsusc.2010.10.051

63- Xiao, B., Wu, G., Wang, T., Wei, Z., Sui, Y., Shen, B., Qi, J., Wei, F., & Zheng, J. (2022). High-entropy oxides as advanced anode materials for long-life lithium-ion batteries. Nano Energy, 95, 106962. https://doi.org/10.1016/j.nanoen.2022.106962

64- Chen, D., Nie, S., Wu, L., Zheng, X., Du, S., Duan, X., Niu, Q., Zhang, P., & Dai, S. (2022a). Metal–tannin coordination assembly route to nanostructured high-entropy oxide perovskites with abundant defects. Chemistry of Materials, 34(4), 1746–1755. https://doi.org/10.1021/acs.chemmater.1c03930

65- Li, J., Hwang, S., Guo, F., Li, S., Chen, Z., Kou, R., Sun, K., Sun, C.-J., Gan, H., Yu, A., Stach, E. A., Zhou, H., & Su, D. (2019). Phase evolution of conversion-type electrode for lithium ion batteries. Nature Communications, 10(1). https://doi.org/10.1038/s41467-019-09931-2

66- Shi, P., Hou, L.-P., Jin, C.-B., Xiao, Y., Yao, Y.-X., Xie, J., Li, B.-Q., Zhang, X.-Q., & Zhang, Q. (2021). A successive conversion–deintercalation delithiation mechanism for practical composite lithium anodes. Journal of the American Chemical Society, 144(1), 212–218. https://doi.org/10.1021/jacs.1c08606

67- Qiu, N., Chen, H., Yang, Z., Sun, S., Wang, Y., & Cui, Y. (2019). A high entropy oxide (MG0.2Co0.2Ni0.2Cu0.2Zn0.2o) with superior lithium storage performance. Journal of Alloys and Compounds, 777, 767–774. https://doi.org/10.1016/j.jallcom.2018.11.049

68- Bui, V. K., Pham, T. N., Hur, J., & Lee, Y.-C. (2021). Review of zno binary and ternary composite anodes for lithium-ion batteries. Nanomaterials, 11(8), 2001. https://doi.org/10.3390/nano11082001

69- Nguyen, T. X., Tsai, C.-C., Patra, J., Clemens, O., Chang, J.-K., & Ting, J.-M. (2022). Co-free high entropy spinel oxide anode with controlled morphology and crystallinity for outstanding charge/discharge performance in lithium-ion batteries. Chemical Engineering Journal, 430, 132658. https://doi.org/10.1016/j.cej.2021.132658

70- Lee, Y.-S., & Ryu, K.-S. (2017). Study of the lithium diffusion properties and high rate performance of tinb6o17 as an anode in lithium secondary battery. Scientific Reports, 7(1). https://doi.org/10.1038/s41598-017-16711-9

71- Zhao, J., Yang, X., Huang, Y., Du, F., & Zeng, Y. (2021). Entropy stabilization effect and oxygen vacancies enabling spinel oxide highly reversible lithium-ion storage. ACS Applied Materials & Interfaces, 13(49), 58674–58681. https://doi.org/10.1021/acsami.1c18362

72- Chen, H., Qiu, N., Wu, B., Yang, Z., Sun, S., & Wang, Y. (2020). A new spinel high-entropy oxide (mg0.2ti0.2zn0.2cu0.2fe0.2)3O4 with fast reaction kinetics and excellent stability as an anode material for lithium ion batteries. RSC Advances, 10(16), 9736–9744. https://doi.org/10.1039/d0ra00255k

73-Shen, L., Lv, H., Chen, S., Kopold, P., van Aken, P. A., Wu, X., Maier, J., & Yu, Y. (2017). Peapod-like li3vo4/n-doped carbon nanowires with pseudocapacitive properties as advanced materials for high-energy lithium-ion capacitors. Advanced Materials, 29(27), 1700142. https://doi.org/10.1002/adma.201700142

74- Ngamchuea, K., Eloul, S., Tschulik, K., & Compton, R. G. (2014). Planar diffusion to macro disc electrodes—what electrode size is required for the Cottrell and Randles-Sevcik equations to apply quantitatively? Journal of Solid State Electrochemistry, 18(12), 3251–3257. https://doi.org/10.1007/s10008-014-2664-z

75- Wang, D., Jiang, S., Duan, C., Mao, J., Dong, Y., Dong, K., Wang, Z., Luo, S., Liu, Y., & Qi, X. (2020). Spinel-structured high entropy oxide (FeCoNiCrMn)3o4 as anode towards superior lithium storage performance. Journal of Alloys and Compounds, 844, 156158. https://doi.org/10.1016/j.jallcom.2020.156158

76- Wang, L., Mercier, D., Zanna, S., Seyeux, A., Laurent-Brocq, M., Perrière, L., Guillot, I., & Marcus, P. (2020). Study of the surface oxides and corrosion behaviour of an equiatomic cocrfemnni high entropy alloy by XPS and TOF-Sims. Corrosion Science, 167, 108507. https://doi.org/10.1016/j.corsci.2020.108507

77- Bayraktar, D. O., Lökçü, E., Ozgur, C., Erdil, T., &; Toparli, C. (2022). Effect of synthesis environment on the electrochemical properties of $(FeMnCrCoZn)_3O_4$ high-entropy oxides for li-ion batteries. International Journal of Energy Research, 46(15), 22124–22133. https://doi.org/10.1002/er.8749

78- Deiss, E. (2005). Spurious chemical diffusion coefficients of Li+ in electrode materials evaluated with Gitt. Electrochimica Acta, 50(14), 2927–2932. https://doi.org/10.1016/j.electacta.2004.11.042

79- Augustyn, V., Simon, P., & Dunn, B. (2014). Pseudocapacitive oxide materials for high-rate electrochemical energy storage. Energy &; Environmental Science, 7(5), 1597. https://doi.org/10.1039/c3ee44164d

80- Wang, J., Polleux, J., Lim, J., & Dunn, B. (2007). Pseudocapacitive contributions to electrochemical energy storage in tio2 (anatase) nanoparticles. The Journal of Physical Chemistry C, 111(40), 14925–14931. https://doi.org/10.1021/jp074464w

81- Rho, Y. H., & Kanamura, K. (2004). Li+ ion diffusion in li4ti5o12 thin film electrode prepared by PVP sol–gel method. Journal of Solid State Chemistry, 177(6), 2094–2100. https://doi.org/10.1016/j.jssc.2004.02.018

82- Deiss, E. (2002). Spurious potential dependence of diffusion coefficients in Li+ insertion electrodes measured with Pitt. Electrochimica Acta, 47(25), 4027–4034. https://doi.org/10.1016/s0013-4686(02)00363-8